BULLETIN DE L'ASSOCIATION MINERALOGIQUE DU CANADA
THE CANADIAN MINERALOGIST
JOURNAL OF THE MINERALOGICAL ASSOCIATION OF CANADA

Volume 35 February 1997 Part 1

The Canadian Mineralogist
Vol. 35, pp. 1-21 (1997)

PLATINUM-GROUP MINERALS IN GOLD-BEARING PLACERS ASSOCIATED WITH THE VELUĆE OPHIOLITE COMPLEX, YUGOSLAVIA

SAŠA KRSTIĆ*

Department of Mineralogy and Crystallography, University of Belgrade, Djušina 7, 11 000 Belgrade, Yugoslavia

MAHMUD TARKIAN

Institute of Mineralogy and Petrology, University of Hamburg, Grindelallee 48, D-20146 Hamburg, Germany

ABSTRACT

The first comprehensive investigation of the platinum-group minerals (PGM) in the gold-bearing placers associated with the Veluće ophiolite complex, Yugoslavia, has shown Ru–Os–Ir and Pt–Fe alloys as the main mineral phases, in the approximate ratio 2:1. A variety of PGM included in individual grains of Ru–Ir–Rh and Pt–Fe alloys are represented by alloys in the systems Ru–Os–Ir, Ru–Ir–Pt, Ir–Os–Rh and Pt–Cu ± (Sb) as well as Rh–Pd and Rh–Ru arsenides, laurite, hollingworthite, irarsite, sperrylite, keithconnite, Pd antimonides, iridarsenite(?) $(Ir,Rh,Pt)(As,Te)_2$, unnamed $(Ru,Rh,Ir)(Te,Sb,As)_2$ and ruthenium oxide(?). Only platarsite is found as an inclusion in a discrete irarsite aggregate. Inclusions of PGM within Ru–Os–Ir and Pt–Fe alloys were trapped either as already solidified mineral grains or they crystallized from trapped, PGE-rich liquid droplets. Likewise, crystallographically oriented intergrowths among PGM also indicate their origin by exsolution from solid solutions. Textural and compositional evidence suggests crystallization of the PGM at magmatic conditions with limited replacement of the primary Ru–Os–Ir alloys by laurite, hollingworthite, irarsite and ruthenium oxide(?). The resemblance of compositions of the PGM in chromitites with those in the placers indicates the ultramafic suite of the ophiolite complex as the likely source for the alluvial PGM mineralization. It appears that most of the PGM precipitated directly from the silicate melt under relatively low $f(S_2)$ but notable contributions of As, Sb and Te in deposition of the platinum-group elements (PGE).

Keywords: platinum-group minerals, electron microprobe, placers, origin, ophiolite complex, Veluće, Yugoslavia.

SOMMAIRE

Nous présentons les résultats de la première étude compréhensive des minéraux du groupe du platine dans les alluvions aurifères associées au complexe ophiolitique de Veluće, en Yougoslavie. Nous y avons trouvé les alliages à Ru–Os–Ir and Pt–Fe comme phases principales, dans un rapport d'environ 2:1. Il y a aussi une variété de minéraux inclus dans les grains de ces alliages, dont des alliages à Ru–Os–Ir, Ru–Ir–Pt, Ir–Os–Rh et Pt–Cu ± (Sb), de même que des arséniures de Rh–Pd et de Rh–Ru,

---

* Present address: Department of Geology, Earth Science Centre, University of Toronto, 22 Russell Street, Toronto, Ontario M5S 3B1. *E-mail address*: sasha@zircon.geology.utoronto.ca.

laurite, hollingworthite, irarsite, sperrylite, keithconnite, des antimoniures de Pd, iridarsenite(?) (Ir,Rh,Pt)(As,Te)$_2$, la phase sans nom (Ru,Rh,Ir)(Te,Sb,As)$_2$, et l'oxyde de ruthénium(?). La platarsite seule est présente comme inclusion dans les agrégats de grains d'irarsite. Ces inclusions minérales ont été incluses dans les alliages soit sous forme de cristaux déjà formés, soit sous forme de gouttelettes de liquide enrichi en éléments du groupe du platine. De même, la présence d'intercroissances cristallographiquement orientées impliquant ces minéraux indique une origine par exsolution à partir de solutions solides. D'après l'évidence texturale et compositionnelle, il y aurait eu cristallisation des minéraux du groupe du platine à une température magmatique, suivie de remplacement local de l'alliage Ru–Os–Ir par laurite, hollingworthite, irarsite et oxyde de ruthénium(?). Les compositions de ces minéraux dans les chromitites et les alluvions aurifères se ressemblent; le cortège ultramafique du massif ophiolitique en serait donc leur source probable. Dans la plupart des cas, les minéraux ont probablement été précipités directement à partir d'un magma silicaté sous conditions de fugacité de soufre relativement faible, avec la participation des éléments As, Sb et Te.

(Traduit par la Rédaction)

Mots-clés: minéraux du groupe du platine, microsonde électronique, alluvions aurifères, origine, complexe ophiolitique, Veluće, Yougoslavie.

INTRODUCTION

The placers associated with the Veluće ophiolite complex in Yugoslavia, which contain platinum-group minerals (PGM) and gold, are the first well-established occurrence of alluvial PGM in the Balkan Peninsula. These placers were exploited for gold in the early part of the century, but exact production is not known; however, remains of the old working could be traced back in the Middle Ages (Popević 1991). In spite of intensive exploration for gold between 1918 and 1940, little attention was paid to the PGM.

The detailed search for the PGM in the area began in the 1950s. Alluvial prospecting in the Srebrenica – Pasjak – Omašnica river system, which drains the ultramafic bedrock, revealed the presence of PGM and gold in approximately a 1:1 ratio (Pašić & Maksimović 1952). The limited studies of the nuggets of PGM collected showed that iridium and native platinum are the main phases in the placers (Pašić & Maksimović 1952).

A recent mineralogical investigation of some PGM nuggets from that collection has been carried out using energy-dispersion spectrometry. Analysis of eight composite PGM nuggets has revealed the presence of Os–Ir–Ru alloy, isoferroplatinum, irarsite and molybdenite(?) (Maksimović 1992; pers. comm. 1993).

Renewed interest in platinum metals in recent years and a discovery of lode PGM occurrences from chromitites in the Veluće ophiolite complex (Krstić 1993) led us to examine earlier results of the placer PGM in greater detail. This paper provides the composition of PGM nuggets collected previously by Pašić & Maksimović (1952) and addresses the question of the origin of the alluvial PGM assemblages.

GEOLOGICAL SETTING

The Veluće ophiolite complex, located in central Serbia, Yugoslavia, is approximately 5 × 1.5 km in size. Host rocks of the complex comprise Paleozoic schists (mica schist, gneiss, phyllite) and Cretaceous flysh sediments (sandstone, limestone, argillite, conglomerate), which transgressively overlie both the schists and the ophiolite complex (Fig. 1). The complex belongs to the Inner Dinaric ophiolite zone (also called the Vardar zone), which forms part of the eastern domain of the Mediterranean ophiolite belt. This zone is widely believed to represent a refractory part of depleted upper mantle, formed in an area similar to a marginal sea or in a narrow oceanic basin (Karamata *et al.* 1980). The ophiolitic rocks were emplaced either as ultramafic diapirs or through obduction of oceanic crust during the Middle to Late Jurassic (Karamata *et al.* 1980, Maksimović 1981, Karamata 1988).

The geology of the complex has been described by Pašić & Maksimović (1952), Popević (1990, 1991) and Krstić (1993). The complex occurs as an E–W-oriented antiform and is largely composed of tectonized harzburgite interlayered with dunite. Both harzburgite and dunite are massive in the central part, but commonly display schistosity along faults and near their margins, particularly at the contact with the overlying gabbro and diabase units. These, along with sedimentary rocks, are distributed at the western and southern margins of the complex and lie in fault contact with harzburgite (Fig. 1).

The ultramafic rocks have been strongly serpentinized. In addition, pervasive hydrothermal alteration produced silificified and carbonatized serpentinite at the northern margin, toward the younger Neogene sediments. Owing to intensive weathering of the ultramafic units, a crust approximately 3000 m long and up to 100 m wide has formed, which contains minor showings of nickel-bearing laterite.

Chromitite pods are restricted to the dunite and derived serpentinite. Alternations of discontinuous bands of disseminated to massive chromitite and dunite are common in the Veluće complex. The thickness of the bands typically ranges from 2 to 10 cm.

Krstić (1993) reported the absence of significant variation in the composition of chromite. It is Cr-rich (55.2–65.8 wt.% Cr_2O_3) and Al-poor (5.4 to 12.3 wt.% Al_2O_3); Al and Cr display a negative correlation, typical of podiform chromite (Thayer 1970, Dick & Bullen 1984). The range of Mg/(Mg + Fe^{2+}) values is between

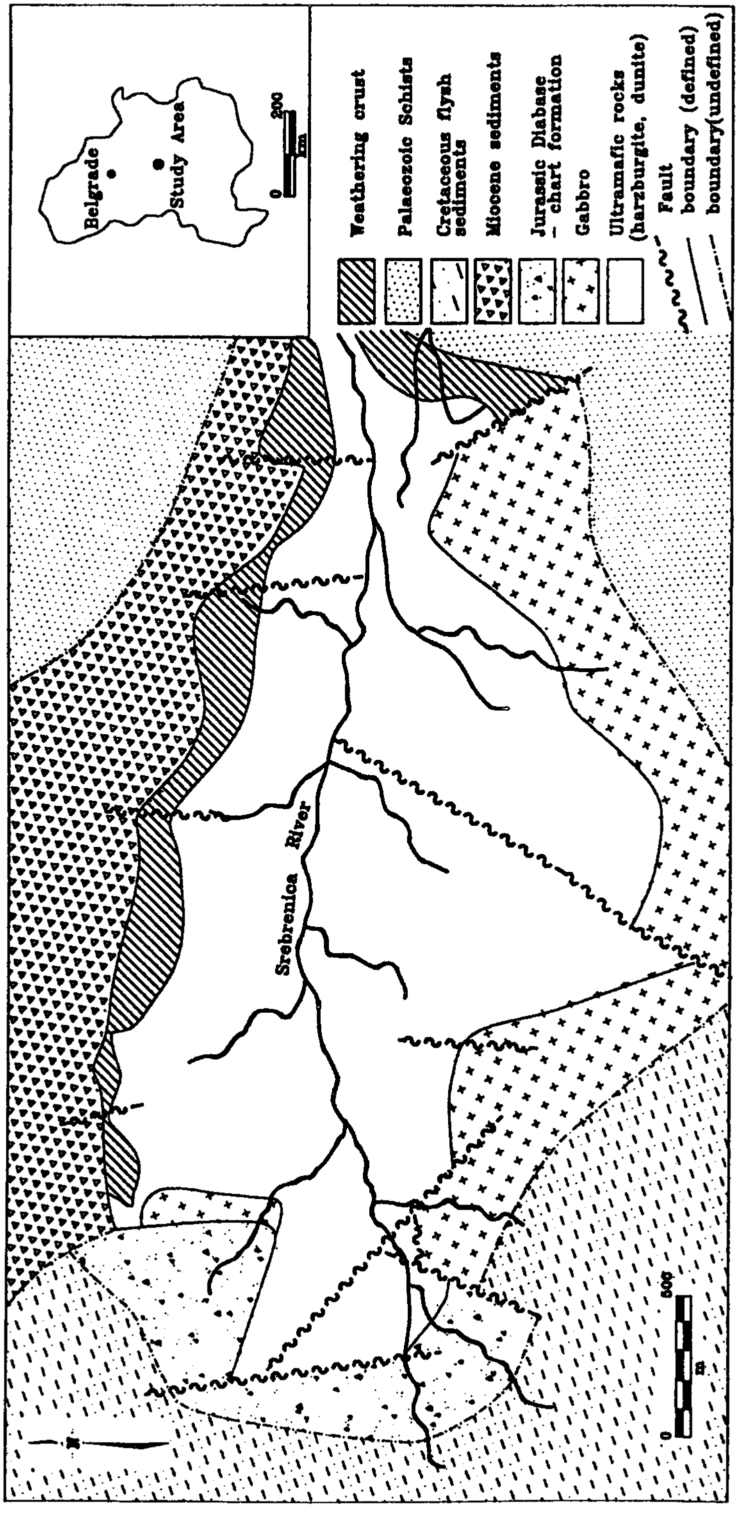

FIG. 1. Geology of the Veluće area, simplified after Pašić & Maksimović (1952) and Popević (1990, 1991).

0.38 (accessory chromite) and 0.62 (massive chromitite); this probably reflects the tendency for chromite and olivine to re-equilibrate under high-temperature, subsolidus conditions, resulting in a lower Mg# for chromite (*e.g.*, Irvine 1965, Roeder & Campbell 1985).

LODE OCCURRENCES OF PGM

The presence of primary PGM mineralization in the podiform chromitites has been noted by Krstić (1993). A total of 16 PGM grains have been found, occurring as both inclusions in chromite and, more rarely, in the serpentinized silicate matrix. The PGM discovered include alloys (osmian ruthenium, iridian osmian ruthenium, rutheniridosmine and iridian ruthenian osmium), sulfarsenides (irarsite, ruarsite and platarsite) and a sulfide (laurite). The euhedral nature of the PGM locked in chromite indicates their crystallization from the silicate melt, before or contemporaneously with the chromite host. The predominance of the Ru–Os–Ir alloy in the PGM assemblages and the paucity of base-metal sulfides in the Veluće chromitite led to the conclusion that chromite and PGM were precipitated from S-impoverished parental liquids (Krstić 1993).

SAMPLES AND ANALYTICAL TECHNIQUES

In the course of an exploration program for chromite and platinum in the Veluće area (Pašić & Maksimović 1952), more than 1000 grains of PGM and gold were recovered from stream and terrace sediments along the Srebrenica river and its tributaries. The rather shallow (up to 0.5 m) pebbly and sandy sediments from the stream channel were panned, with a sampling interval of about 200 m. Along with collections of the heavy-mineral concentrates from river sand and gravels, 20 pits were dug in the narrow (up to 10 m) alluvial bars on the river banks. Gravel and weathered ultramafic bedrock exposed in the pits were sieved and panned. The PGM and gold nuggets were hand-picked from a pan as well as under a stereo microscope after refining the heavy-mineral fraction in the laboratory by repeated panning and processing in a Franz magnetic separator (Pašić & Maksimović 1952).

Through the kindness of Prof. Z. Maksimović, several hundred PGM and gold nuggets were obtained from his collection. They have been examined with a stereo microscope, and a selection of about 160 nuggets was mounted in araldite for a reflected-light investigation and electron-microprobe analysis. A total of 61 PGM nuggets were analyzed.

Compositions of the PGM and gold were determined by a Cameca Camebax Microbeam wavelength-dispersion microprobe at the Department of Mineralogy and Petrology, University of Hamburg. The acceleration voltage was 20 kV, with a beam current of 20 nA and a beam diameter of less than 1 μm. The following X-ray lines were used: Pt*L*α, Ir*L*α, Os*M*α, Ru*L*α, Rh*L*α, Pd*L*β, Fe*K*α, Ni*K*α, Cu*K*α, S*K*α, As*K*α, Te*L*α, Sb*L*α, Bi*M*β, Ag*L*α, Au*M*α, Hg*M*α. Pure elements (Pt, Ir, Os, Ru, Rh, Pd, Fe, Ni, Bi, Ag and Au), as well as pyrite (S), stibnite (Sb), covellite (Cu), cinnabar (Hg), synthetic PdBiTe (Te) and AsGe (As), were used as standards. Matrix correction were applied using the CAMECA PAP software. The detection limit for all elements is 0.1 wt.%.

TABLE 1. PLATINUM - GROUP MINERALS IN VELUCE PLACERS

Mineral	Minor constituents	Abundance*
Ru-Os-Ir alloy		
Ruthenium Ru (Os,Ir)	Pt, Rh, Cu	XXX
Osmium Os (Ru,Ir)	Pt, Rh, Cu	XX
Rutheniridosmine (Ir,Os,Ru)	Pt, Rh, Fe, Cu	X
Pt-Fe alloy		
Isoferroplatinum Pt_3Fe	Rh, Ir, Cu, Sb	XXX
Native platinum Pt	Ir, Fe, Cu	X
Ru-Ir-Rh alloy		
Ruthenium Ru (Ir,Rh)	Os, Pt	X
Ru-Ir-Pt alloy		
Unnamed Ru-rich alloy Ru (Pt,Ir)	Rh, Os, Fe, Cu	XX
Iridium Ir (Ru,Pt)	Rh, Os, Fe, Cu	X
Platinum Pt (Ru,Ir)	Rh, Os, Fe, Cu	X
Ir-Os-Rh alloy		
Iridium Ir (Os,Rh)	Pt, Ru, Fe, Cu	X
Osmium Os (Ir,Rh)	Pt, Ru, Fe, Cu	X
Pt-Cu±Sb		
Pt_3Cu	Rh, Ru, Ni, Fe	X
Pt-Cu-Sb	Pd, Rh	X
$Pt_3(Sb,Cu)$	Rh, Fe, As	X
Sulfides		
Laurite RuS_2	Os, Rh, Ir, As	XXX
Sulfarsenides		
Hollingworthite RhAsS	Ru, Ir, Pt, Os	XX
Irarsite IrAsS	Rh, Ru, Pt	XX
Platarsite PtAsS	Ir, Ru	X
Arsenides		
Sperrylite $PtAs_2$	Ir, Rh, Te	XX
$(Rh,Pd)_2As$	Pt, Te, Sb	XX
(Rh,Ru)As	Ir, Pt	XX
Iridarsenite (?) $(Ir,Rh,Pt)(As,Te)_2$	Ru, Sb, Os, Cu	X
Telurides		
Keithconnite Pd_3Te	Rh, Pt, Cu	X
$(Ru,Rh,Ir)(Te,Sb,As)_2$	Pt, Bi	X
Antimonides		
Pd-Sb	Pt, Cu, As	XX
Oxides		
RuO_2 (?)	Ir, Os, Fe, Hg	X

* xxx = most common; xx = common; x = rare.

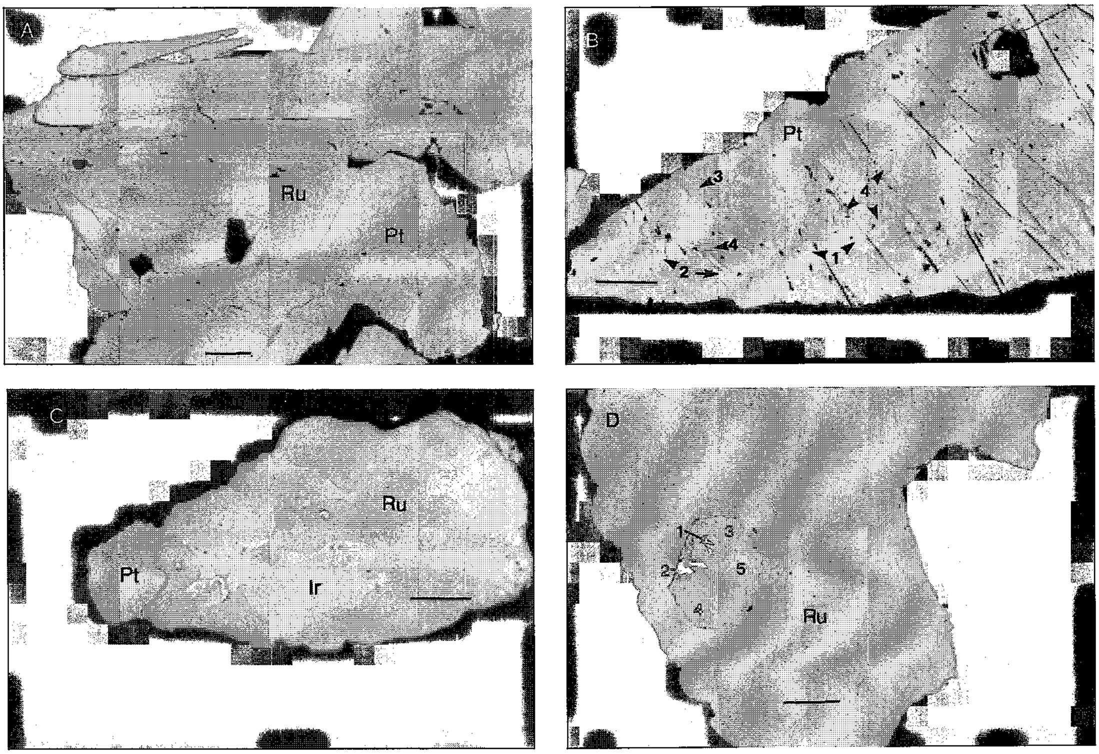

FIG. 2. Reflected-light photomicrographs of PGM. A. An intergrowth of prismatic crystals of the Ru–Os–Ir alloy (Ru) with Pt–Fe alloy (Pt). B. Ru–Ir–Pt (1) and Ru–Ir–Rh (2) alloys, Rh–Pd arsenide (3) and keithconnite (4) included in the host Pt–Fe alloy (Pt). C. An intergrowth of Ru–Ir–Pt alloy (Ir) and rutheniridosmine (Ru) with an attached grain of Pt–Fe alloy (Pt). D. A polyphase inclusion of sperrylite (1), Rh–Ru arsenide (2), Rh–Pd arsenide (3), Pt–Cu–Sb alloy (4) and Pt–Fe alloy (5), hosted by Ru–Os–Ir alloy (Ru). Bar scale: 100 μm in A–C, 50 μm in D.

MINERAL ASSEMBLAGES

The species of PGM in placer deposits of the Veluće area and their relative frequency are listed in Table 1. The PGM found as discrete phases are Ru–Os–Ir and Pt–Fe alloys and irarsite (one grain). All other observed PGM phases occur as exsolution-related domains and inclusions in these alloys, as well as products of replacement along grain margins. The relative proportion of Ru–Os–Ir and Pt–Fe alloys is approximately 2:1.

Ru–Os–Ir alloy

Ru–Os–Ir alloy is the most abundant species encountered. Grains range in size from a few μm up to 5 mm. They usually occur as discrete, irregular to subhedral and equidimensional crystals with a partly rounded outline. Rarely, tiny spindle-like grains, exsolution-related blebs and laths of Ru–Os–Ir alloy have been found in Ru–Ir–Pt and Pt–Fe alloys. They are present either as single phases (Fig. 2A) or associated with Rh–Pd arsenide.

A common feature of the Ru–Os–Ir alloy is the presence of other PGM and chromite as inclusions and marginal replacements. Besides PGE alloys, inclusions are represented by Rh–Pd arsenide, Rh–Ru arsenide, sperrylite, Pd antimonides, laurite, an unnamed $(Ru,Rh,Ir)(Te,Sb,As)_2$ phase, and chromite. Solitary and polyphase inclusions show either random distribution with no preferred crystallographic orientation with respect to the host Ru–Os–Ir alloy, or an arrangement along cleavages.

The Ru–Os–Ir alloy exhibits a relatively large compositional range (Table 2). According to revised nomenclature by Harris & Cabri (1991), most grains correspond to ruthenium with variable contents of Os and Ir (Fig. 3). However, following the proposed approach for plotting analytical data in a triangular diagram (Harris & Cabri 1991), compositions of the Ru–Os–Ir alloy, found as both one discrete grain and exsolution lamellae and blebs in a grain of Pt–Fe alloy, fall in the miscibility gap (Harris & Cabri 1973) owing to the high Pt and Rh contents, which vary from 11.63 to 22.31 at.% (Pt + Rh). These alloys actually belong to the system Ru–Os–Ir with significant impurities

TABLE 2. SELECTED ELECTRON-MICROPROBE DATA OF PGE ALLOYS

Analysis No.	3	19	55	64	174	54	11	199	114	26	103	104	132
Pt wt. %	1.65	9.10	3.42	12.39	86.21	87.60	72.75	3.59	39.83	49.28	10.16	1.01	85.98
Ir	23.12	27.12	33.53	50.08	0.49	<0.10	4.20	35.98	21.28	13.25	51.92	34.10	<0.10
Os	30.80	15.27	38.45	16.97	<0.10	<0.10	2.02	1.95	7.56	4.06	25.91	59.65	<0.10
Ru	44.24	45.08	21.17	12.91	0.28	0.19	7.94	44.45	20.26	28.70	4.74	2.09	0.26
Rh	0.78	3.72	2.86	6.64	2.23	0.33	5.89	13.27	8.39	3.99	5.50	2.43	0.35
Pd	<0.10	<0.10	<0.10	<0.10	0.11	<0.10	0.17	<0.10	<0.10	<0.10	<0.10	<0.10	<0.10
Fe	<0.10	<0.10	<0.10	0.42	8.30	4.93	6.04	0.13	1.36	0.47	0.27	<0.10	0.21
Cu	0.20	0.25	0.35	0.44	1.81	4.44	1.04	0.31	0.52	0.32	0.59	0.34	11.82
Ni	<0.10	<0.10	<0.10	<0.10	0.14	0.37	0.12	<0.10	<0.10	<0.10	<0.10	<0.10	0.43
As	<0.10	<0.10	<0.10	<0.10	<0.10	<0.10	<0.10	<0.10	<0.10	<0.10	<0.10	<0.10	<0.10
Sb	<0.10	<0.10	<0.10	<0.10	<0.10	1.75	<0.10	<0.10	<0.10	<0.10	<0.10	<0.10	<0.10
Total	100.79	100.54	99.78	99.85	99.57	99.61	100.17	99.68	99.21	100.07	99.09	99.62	99.05
Atomic proportions													
Pt	1.14	6.19	2.76	10.24	2.72	2.86	2.23	2.32	30.51	37.19	9.08	0.94	2.74
Ir	16.28	18.71	27.39	42.03	0.02	-	0.13	23.64	16.54	10.15	47.15	32.50	-
Os	21.92	10.64	31.74	14.40	-	-	0.06	1.29	5.94	3.14	23.78	57.46	-
Ru	59.20	59.14	32.89	20.60	0.02	0.01	0.47	55.55	29.96	41.82	8.19	3.78	0.02
Rh	1.02	4.80	4.36	10.40	0.13	0.02	0.34	16.29	12.18	5.71	9.32	4.33	0.02
Pd	-	-	-	-	0.01	-	0.01	-	-	-	-	-	-
Fe	-	-	-	1.21	0.92	0.56	0.65	0.29	3.64	1.24	0.84	-	0.02
Cu	0.43	0.52	0.86	1.11	0.18	0.44	0.10	0.61	1.23	0.73	1.63	0.98	1.16
Ni	-	-	-	-	0.01	0.09	0.01	-	-	-	-	-	0.04
As	-	-	-	-	-	-	-	-	-	-	-	-	-
Sb	-	-	-	-	-	0.09	-	-	-	-	-	-	-

3 - a discrete grain of Ru-Os-Ir alloy; 9 - exsolution blebs of Ru-Os-Ir alloy, accompanied by Rh-Pd arsenide within a grain of Pt-Fe alloy; 55 - inclusions of Ru-Os-Ir alloy in laurite, all locked in a complex polymineralic grain made of Ru-Os-Ir and Pt-Fe alloys; 64 - exsolution laths of Ru-Os-Ir alloy in Pt-Fe alloy; 174 - a lamella of Pt-Fe alloy in Ru-Os-Ir alloy; 54 - Pt-Fe alloy as part of a polyphase inclusion in a grain of Ru-Os-Ir alloy (Fig. 2D); 11 - PGE-bearing Pt-Fe alloy in a mirmecitic intergrowth with isoferroplatinum; 199 - an anhedral grain of Ru-Ir-Rh alloy in Pt-Fe alloy (Fig. 2B); 114 - an anhedral grain of Ru-Pt-Ir alloy at the margin of Pt-Fe alloy; 26 - exsolution blebs of Ru-Pt-Ir alloy within a grain of Pt-Fe alloy; 103, 104 - irregular intergrowths of Ir-Os-Rh alloy; 132 - a irregular grain of Pt_3Cu as part of a polymineralic inclusion comprising Pt-Cu, Pt-Cu-Sb and Ru-Os-Ir alloys, and Rh-Ru and Rh-Pd arsenides, all included in Ru-Os-Ir alloy.

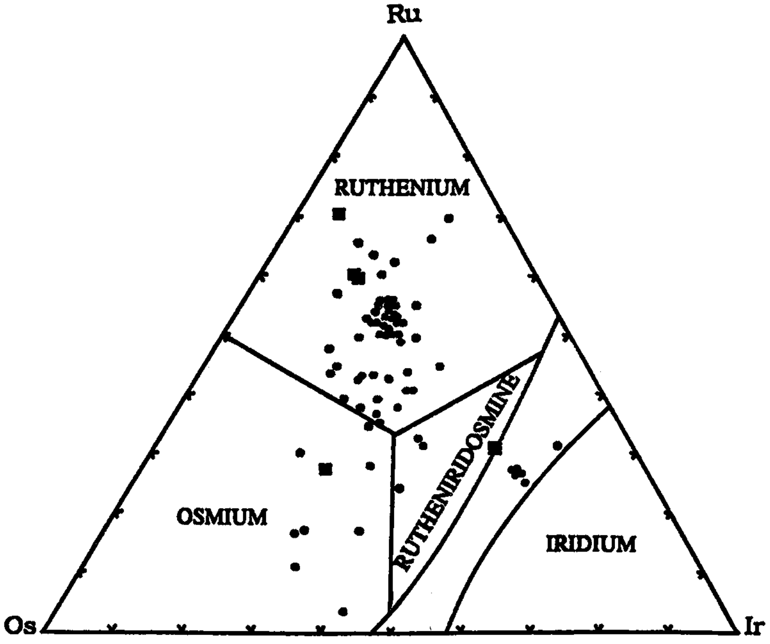

FIG. 3. Compositions of alloys (at.%) in the system Ru–Os–Ir, with the miscibility gap drawn according to Harris & Cabri (1973); ● placers (this study); ■ inclusions in chromite (Krstić 1993).

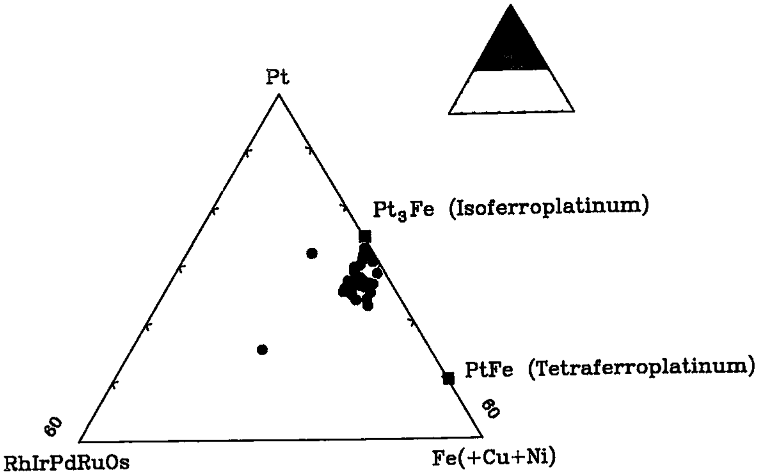

FIG. 4. Compositions of Pt–Fe alloy (at.%) plotted in the diagram Pt – (Fe + Ni + Cu) – (Rh + Ir + Pd + Ru + Os).

of Pt and Rh. Similar compositions were attributed by Augé & Maurizot (1995) to Os–Ir–Ru alloy in PGE mineralization from New Caledonia. Other minor elements encountered are Cu (0.39–1.45 at.%), Fe (<0.1–2.28 at.%) and Ni (up to 0.17 at.%). Palladium is almost always below the detection limit; it was detected in a few cases, with a maximum content of 0.14 at.%. These values are comparable with results obtained from primary Ru–Os–Ir alloy in chromitite (Krstić 1993). The most striking difference is the predominance of Cu over Fe in grains of Ru–Os–Ir alloy from this study.

The compositions of the Ru–Os–Ir alloy also partly reflect the nature of the adjacent PGM. Discrete and inclusion-free grains of Ru–Os–Ir alloy show lower Pt and Rh contents than grains that coexist with Pt–Fe alloy and Rh–Pd arsenides, respectively. This could be related to the composition of the ore-forming system from which the PGM have crystallized, because a medium enriched in Pt and Rh could have produced Pt and Rh enrichment in the Ru–Os–Ir alloy and the appearance of discrete Pt- and Rh-bearing minerals in composite grains.

The Ru–Os–Ir alloy, with a broad variation in proportion of Ru, Os and Ir, commonly occurs as a discrete phase in placers, *e.g.*, the Territory of Papua – New Guinea (Harris & Cabri 1973), Witwatersrand (Feather 1976), Sorashigava, Japan (Stumpfl & Tarkian 1976, Tarkian 1987), Tasmania (Ford 1981, Peck *et al.* 1992), the Urals (Tarkian 1987), southeastern Kalimatan, Borneo (Burgath 1988), Burma (Hagen *et al.* 1990), New Caledonia (Augé & Maurizot 1995). On the other hand, included laths and exsolution-induced blebs of Ru–Os–Ir alloy in Pt–Fe grains are either Os-rich (Cabri *et al.* 1981, Augé & Legendre 1992, Weiser & Schmidt-Thomé 1993) or both Os-and Ir-rich (Toma & Murphy 1977, Törnroos & Vuorelainen 1987, Cabri & Genkin 1991, Slansky *et al.* 1991). Contrary to these findings, alloy grains examined here are mostly Ru-rich regardless of their mode of occurrence, which probably reflects a Ru-enriched source of the PGM.

Pt–Fe alloy

As the second most abundant mineral in the samples, Pt–Fe alloy typically occurs as single irregular grains with partly rounded or scalloped outlines or as inclusions in Ru–Os–Ir alloy. Tiny oriented exsolution-induced lamellae and blebs in Ru–Os–Ir alloy and symplectitic intergrowths with Ru–Ir–Os alloy have also been observed locally. The grains are between 200 μm and 2 μm across, whereas the diameter of the inclusions of Pt–Fe alloy in Ru–Os–Ir alloy varies from a few up to 100 mm. Grains of Pt–Fe alloy may contain many different types of inclusions, *e.g.*, Ru–Os–Ir, Ru–Ir–Pt and Ru–Ir–Rh alloys, as well as Rh–Pd arsenide, laurite, hollingworthite, Pd antimonides and keithconnite.

The composition of Pt–Fe alloy (Table 2) appears to be homogeneous, stoichiometrically close to isoferroplatinum (Fig. 4). The Pt content varies from 63.14 to 73.47 at.%, with an average amount of 68.5 at.%. Rhodium and Ir are invariably recorded in significant quantities, and attain 6.28 and 3.02 at.%, respectively. A clear negative correlation between Rh and Pt (Fig. 5) indicates the substitution of Rh for Pt in isoferroplatinum, similar to findings of Augé & Maurizot (1995). Ruthenium shows a rather low concentration (<0.7 at.%) despite the common presence of Ru–Os–Ir alloy inclusions in Pt–Fe alloy. The average amount of Pd is 0.46 at.%, with a maximum of 3.37 at.%, whereas Os is almost invariably below its detection limit. In one case, however, a grain of Pt–Fe alloy containing appreciable concentrations of Ru, Rh, Ir, Os and Pd (ΣRu,Rh, Ir,Os,Pd = 25 at.%) has been found. This isotropic, bright-white alloy occurs in a

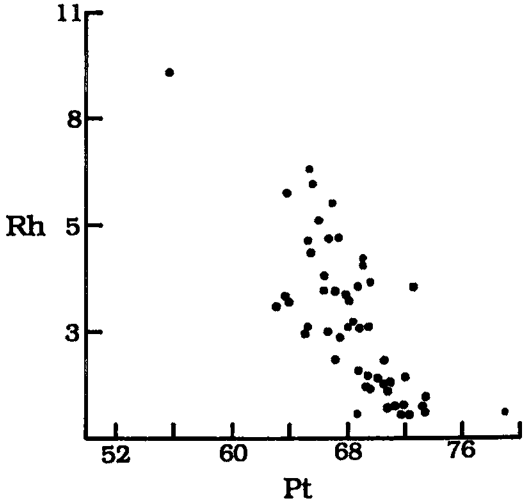

FIG. 5. Relation between Rh and Pt concentrations (at.%) in Pt–Fe alloy.

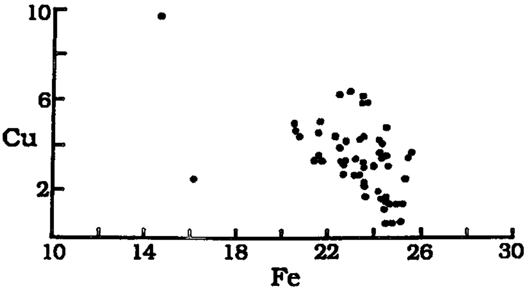

FIG. 6. Relation between Cu and Fe concentrations (at.%) in Pt–Fe alloy.

composite grain forming a symplectitic intergrowth with isoferroplatinum, and is in contact with a grain of Ru–Os–Ir alloy. A Pt–Fe alloy of similar composition was identified by Ford (1981) and Peck *et al.* (1992) in placers from Adamsfield, Tasmania.

The abundance of Fe varies between 14.74 and 25.67 at.%, the most commonly encountered composition being in the range of 23–25 at.%. The Cu content varies from <0.10 to 10.72 at.%, and the observed negative correlation between Cu and Fe (Fig. 6) indicates a solid solution between Pt_3Fe and Pt_3Cu. In addition, a minor content of Ni (<1 at.%) and traces of As were detected in the Pt–Fe alloy. Concentrations of Sb are usually low (<1 at.%), although a grain of Pt–Fe alloy in a polyphase inclusion with sperrylite, Pt–Cu–Sb alloy, Ru–Rh arsenide and Rh–Pd arsenide within a Ru–Ir–Os alloy carries 2.30 at.% Sb.

It is interesting to note that single crystals of Pt–Fe alloy devoid of inclusions show no significant compositional differences from those in polycrystalline aggregates. This finding suggests that crystallization of Pt–Fe alloy occurred in an environment with a relatively uniform composition.

The compositions of the Pt–Fe alloy studied here are similar to those from the Durance River, France (Johan *et al.* 1990). In a discussion of compositional variations of Pt–Fe alloy, they noted that PGE mineralization related to Alaskan-type intrusions contains Pt–Fe alloy with the highest concentration of Cu. The present investigation indicates that this kind of enrichment is not atypical of PGM assemblages related to ophiolites; therefore, the use of the composition of the Pt–Fe alloy as a marker of an Alaskan-type source for placer deposits seems to have rather limited promise.

Ru–Ir–Rh alloy

Laths and anhedral grains of Ru–Ir–Rh alloy have been observed as inclusions within a grain of Pt–Fe alloy. They occur either as isolated crystals or attached to an assemblage of Rh–Pd arsenide, keithconnite and Ru–Ir–Pt alloy, all trapped in the host Pt–Fe grain (Fig. 2B). Laths are 2 to 10 μm in width, with a length of up to 60 μm. The crystal size of the subhedral grains varies between 15 × 15 μm and 20 × 30 μm. The composition of all crystals seems to be homogeneous, and no zoning was discovered (Table 2). It corresponds to iridian rhodian ruthenium, with formulae in the range $Ru_{0.53}Ir_{0.26}Rh_{0.13}Os_{0.04}Pt_{0.04}Cu_{0.01}$ – $Ru_{0.56}Ir_{0.24}Rh_{0.16}Pt_{0.02}Os_{0.01}Cu_{0.01}$. Contents of minor elements (Pd, Cu, Fe and Ni) correspond to values recorded in the Ru–Os–Ir alloy.

Natural alloys in the system Ru–Ir–Rh are quite rare. They have been reported in placers from Japan (Urashima *et al.* 1974) and China (Mao & Zhou 1989). The composition of iridian rhodian ruthenium obtained here differs slightly from "iridrhodruthenium" of Mao & Zhou (1989) in its higher content of Ir.

Ru–Ir–Pt alloy

An alloy in the system Ru–Ir–Pt is fairly common and usually associated with grains of Pt–Fe alloy, occurring either as inclusions or on the rims of the host Pt–Fe alloy. The crystal forms of the inclusions vary from anhedral and isometric, drop-like to subhedral, with diameters ranging from 1 to 120 μm (Fig. 2B). Most inclusions represent solitary phases, but locally they are accompanied by Rh–Pd arsenide, keithconnite, Ru–Ir–Rh alloy, Ru–Ir–Os alloy and hollingworthite. Grains of Ru–Ir–Pt alloy along the margins usually are anhedral, with an average size between 20 and 40 μm. In one case, the Ru–Ir–Pt alloy forms intimate, eutectic-like intergrowth with rutheniridosmine (Fig. 2C).

Results of electron-microprobe analyses are given in Table 2. Majority of the grains are Ru-rich and range in composition from $Ru_{0.42}Pt_{0.36}Ir_{0.10}Rh_{0.06}Os_{0.03}Fe_{0.01}Cu_{0.01}$

to $Ru_{0.32}Pt_{0.28}Ir_{0.18}Rh_{0.13}Os_{0.06}Fe_{0.02}Cu_{0.01}$. These compositions fall in the area B (Fig. 7), which represents the compositional range of a Ru-rich phase in the system Ru–Ir–Pt (Harris & Cabri 1991). As these authors suggested, "if a cubic alloy with that composition is found, it would qualify for a new mineral name". However, most analyzed grains have more complicated compositions, and should be plotted in the quaternary system Ru–Ir–Pt–Rh. Only two single inclusions could be considered as true alloy in the system Ru–Ir–Pt, with no significant impurities of Rh and Os.

As shown in Table 2, Os and Rh are invariably present in the grains of Ru–Ir–Pt alloy, and they obviously display significant preference for these alloys over the host Pt–Fe alloy. The Os content reaches 13.55 at.% in an Ir-rich member that is intergrown with rutheniridosmine, whereas the Rh concentration varies from 4.93 to 15.50 at.%. Other elements, such as Fe, Cu and Ni, also have been detected. The concentrations of Fe ranges from 0.7 to 2.5 at.%, whereas those of Cu and Ni are generally close to 1 and 0.2 at.%, respectively.

Natural alloys in the system Ru–Ir–Pt have been found in placers from Sorashigawa, Japan (Tarkian 1987) and Burma (Hagen *et al.* 1990). The composition given by Tarkian (1987) shows no Rh, whereas the chemistry of a Ir-rich alloy reported by Hagen *et al.* (1990) is very similar to that obtained here.

Ir–Os–Rh alloy

Ir- and Os-rich alloy members in the system Ir–Os–Rh occur as a mutual lamellar intergrowth, probably formed by the breakdown of a homogeneous, high-temperature Ir–Os–Rh alloy. This intergrowth hosts inclusions of euhedral laurite up to 200 µm in diameter, whereas Pt–Fe alloy is developed as a marginal replacement.

The compositions of the Ir–Os–Rh alloy (Table 2) are consistent with the presence of a miscibility gap in the ternary system Ir–Os–Rh (Fig. 8), as proposed by Harris & Cabri (1991). The amount of Ir ranges from 50.37 to 32.39 at.%. Consequently, Os exhibits an inverse relationship with Ir, varying from 27.70 to 57.26 at.%. The concentration of Rh is relatively uniform in the Ir-rich alloy (8.35–9.59 at.%), but is lower (up to 4.32 at.%) in the Os-rich member of the Ir–Os–Rh alloy. Absolute abundances of Pt and Ru are consistently higher in the Ir-rich member (9.07 and 8.15 at.%, respectively) than in the Os-rich alloy (0.94 and 3.77 at.%, respectively).

Pt–Cu and Pt–Cu–Sb alloys

These compounds have been found in polyphase inclusions within grains of Ru–Os–Ir alloy. Among these, only the three largest inclusions were amenable

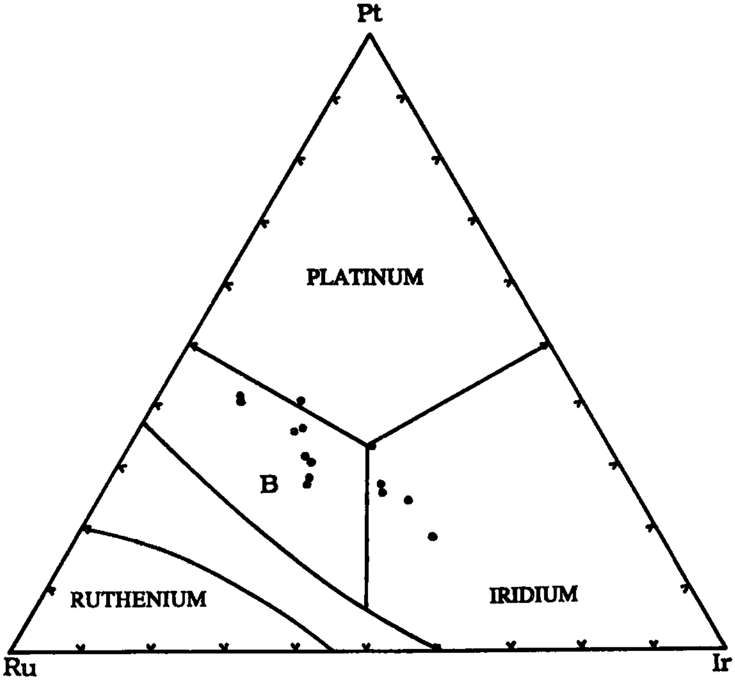

FIG. 7. Compositions of alloys (at.%) in the system Ru–Ir–Pt; the area B and the miscibility gap are drawn according to Harris & Cabri (1991).

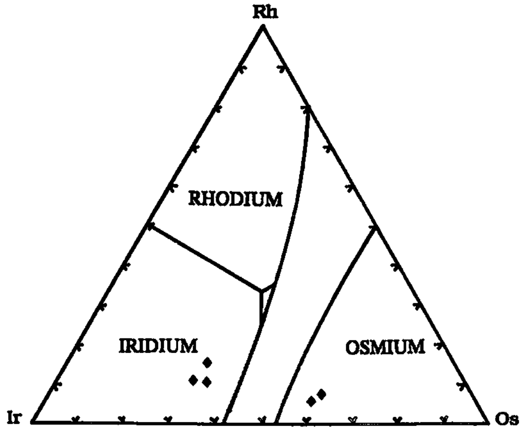

FIG. 8. Compositions of alloys (at.%) in the system Ir–Os–Rh; the miscibility gap is drawn according to Harris & Cabri (1991).

to chemical investigation (Table 2). The alloy Pt_3Cu, associated with Pt–Cu, Pt–Cu–Sb and Ru–Os–Ir alloys and Rh–Ru and Rh–Pd arsenides in a polymineralic inclusion within Ru–Os–Ir alloy, occurs as an anhedral grain 130 μm across and exsolution-induced blebs and rods in the Pt–Cu–Sb alloy. The composition indicates a deficiency in Pt and corresponds to a formula $(Pt_{2.74}Rh_{0.02}Ru_{0.02})_{\Sigma 2.78}(Cu_{1.16}Ni_{0.04}Fe_{0.02})_{\Sigma 1.22}$. A similar phase that had exsolved in isoferroplatinum from Madagascar was described by Augé & Legendre (1992). The composition of this phase differs from that recorded here by the presence of Pd (up to 7 at.%) and minor Au (0.3–0.5 at.%), as well as by higher content of Fe (up to 5 at.%). A Pt–Cu intermetallic phase close to the composition Pt_2Cu_3 was described by Johan *et al.* (1990), whereas Törnroos & Vuorelainen (1987) have reported a Pt–Cu alloy and analogous to hongshiite (PtCu, Ding 1980) and Au- and Rh-bearing Pt–Cu–Fe alloy.

Two grains of Pt–Cu–Sb alloy were analyzed. One occurs as an anhedral grain 70 μm across in the assemblage mentioned above. It is intimately intergrown with Rh–Pd arsenide, Ru–Os–Ir alloy and Rh–Ru arsenide.

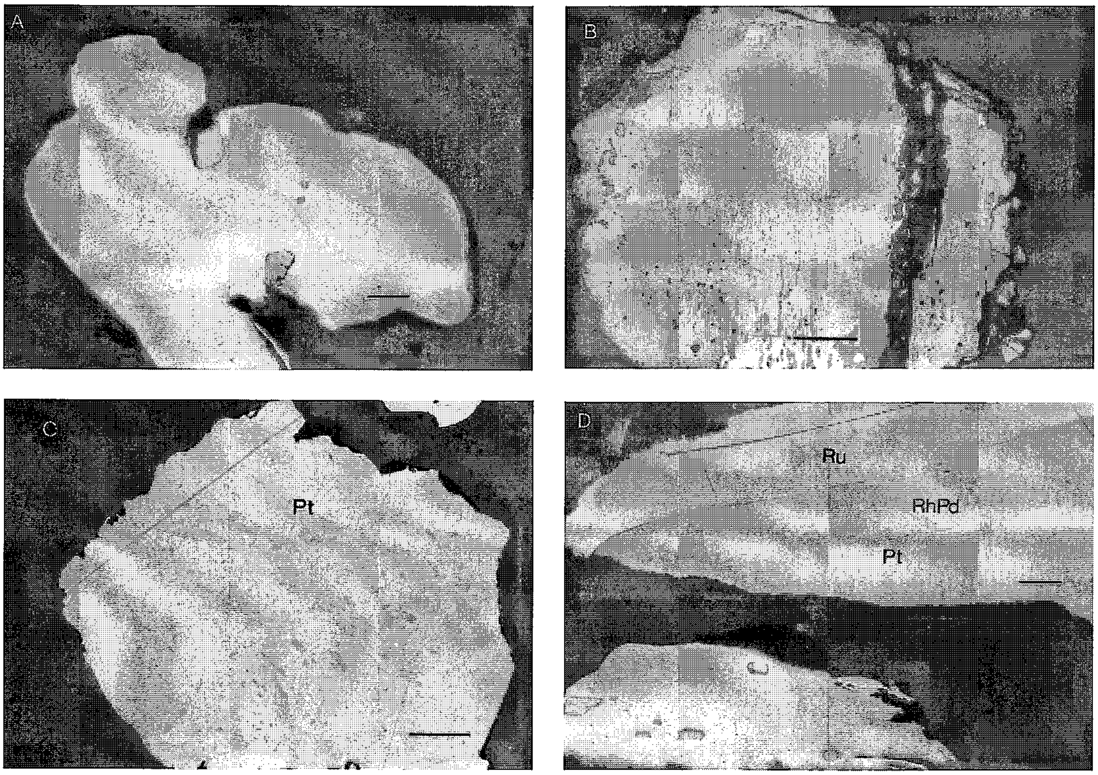

FIG. 9. Reflected-light photomicrographs of PGM. A. Inclusions of laurite (grey) within a grain of Ru–Os–Ir alloy (white). B. A laurite rim (grey) around Ru–Os–Ir alloy (white). C. Exsolution-induced blebs of Rh–Pd arsenide (dark grey) within a grain of Pt–Fe alloy (Pt). D. A globular inclusion of Rh–Pd arsenide (RhPd) attached to a lamella of Ru–Os–Ir alloy (Ru), all trapped within a grain of Pt–Fe alloy (Pt). Bar scale: 100 μm in A–C, 50 μm in D.

The other is hosted by a grain of Ru–Os–Ir alloy, as part of a subhedral inclusion composed of sperrylite, Pt–Fe alloy, Rh–Pd arsenide and Rh–Ru arsenide (Fig. 2D). The chemical compositions are uniform and correspond to formulae in the range $Pt_{0.54}Cu_{0.34}Sb_{0.09}Rh_{0.01}As_{0.01}$ – $Pt_{0.52}Cu_{0.36}Sb_{0.09}Pd_{0.02}Fe_{0.01}$.

An anhedral grain of $Pt_3(Sb,Cu)$ alloy, 45 × 25 μm in size, is associated with sperrylite, Rh–Ru arsenide and native platinum; it forms an irregular inclusion within a grain of Ru–Os–Ir alloy. The composition corresponds to the formula $(Pt_{2.82}Pd_{0.04}Rh_{0.03})_{\Sigma 2.89}(Sb_{0.59}Cu_{0.38}Fe_{0.08}As_{0.05})_{\Sigma 1.10}$. No natural phase of similar composition has been reported to date.

Laurite

Laurite is the only PGE sulfide recorded in the samples. It was found as inclusions in Ru–Os–Ir and Pt–Fe alloys, and occurs mainly as solitary euhedral to anhedral crystals (Fig. 9A) and irregular aggregates. The grain size varies from a few μm to 300 μm across. Laurite has also been identified as a continuous rim along the periphery of grains of Ru–Os–Ir alloy and spindle-like and lenticular grains, disposed along basal planes in the host Ru–Os–Ir alloy. In several cases, an alteration rim of Ru–Os–Ir alloy is optically inhomogeneous and composed of fine-grained laurite accompanied with subordinate irarsite (Fig. 9B).

Representative electron-microprobe data are given in Table 3. No intragrain chemical zoning was found, but laurite exhibits an appreciable compositional variation among the individual grains. Osmium, which shows a negative correlation with Ru, is encountered in a broad range from <0.1 to 33.34 wt.%. Rhodium and Ir were consistently found to be present in laurite. The former is relatively uniformly distributed, varying from 0.8 to 7 wt.%, with a concentration of about 4 wt.% being typical; the latter is in the range of 0.5 to 18 wt.%. The majority of laurite grains show elevated quantities of As (up to 9.39 wt.%) and rather low levels of Pt (up to 1.43 wt.%).

The composition of laurite seems to be strongly influenced by the nature and composition of adjacent PGM phases. For example, euhedral inclusions of laurite in a matrix comprising Os- and Ir-rich members of the Ru–Os–Ir alloy are enriched in Os and Ir, respectively. On the other hand, crystals of laurite set in Ru-rich alloy have little or no Os, whereas Ir displays a variable concentration. Similarly, laurite developed at the margin of a grain of Os-rich alloy usually has a higher content of Os than laurite at the boundary of grains of Ru-rich alloy. With regard to the low average content of Os in laurite (4.2 wt.%), a relatively low $f(S_2)$ in the ore-forming system could be inferred (Legendre & Augé 1986). Abundances of Rh and As in laurite are positively correlated. Enrichment of laurite in these elements is especially significant in crystals that are intergrown with hollingworthite and in solitary grains associated with Rh–Pd arsenide. This is clearly a consequence of locally increased Rh and As activity during laurite precipitation that, apart from influencing its composition, gave rise to Rh- and As-bearing phases. The fact that laurite from the Veluće chromitite carries Rh and As in comparable quantities (Krstić 1993) is evidently very important in an evaluation of its origin in the placers.

Hollingworthite

Hollingworthite is commonly associated with laurite, occurring either at the margin of grains of Ru–Os–Ir alloy or locked in Pt–Fe alloy. Hollingworthite usually appears as a minor, included phase in the laurite host, although several euhedral, single grains of hollingworthite have been found. They range in size from 15 to 150 μm across.

The compositions of hollingworthite (Table 3) show a peculiar deficiency in As compared to ideal formula (RhAsS). This noticeable departure from an As:S ratio of 1 also is characteristic of solitary crystals devoid of laurite.

The hollingworthite examined here represents a component of the hollingworthite – irarsite – ruarsite solid solution. The Ir abundance is in the range of 18 to 32 mol.% IrAsS, whereas the Ru abundance attains 27 mol.% RuAsS. Contrary to reported compositions from other localities (*cf.* Tarkian 1987), the concentration of Pt is relatively low (maximum: 8 mol.% PtAsS), and a noteworthy quantity of Os is observed (up to 5 mol.% OsAsS).

Irarsite

In addition to Ru–Os–Ir and Pt–Fe alloys, irarasite is the only PGM found as a discrete, independent nugget. It occurs as a rounded aggregate approximately 0.4 × 0.5 mm in size. Rarely, anhedral grains of irarasite were found as inclusions in Pt–Fe alloy and as a minor phase, coexisting with laurite in the alteration rim around grains of Ru–Os–Ir alloy.

The representative electron-microprobe-derived composition is given in Table 3. The composition of irarsite varies from almost pure irarsite (IrAsS) with negligible quantities of Pt, Ru and Os (the irarsite nugget) to a component in the irarsite–hollingworthite solid solution (the inclusions in the Pt–Fe alloy). The latter range in composition from $(Ir_{0.53}Rh_{0.33}Ru_{0.08}Pt_{0.07})_{\Sigma 1.01}(As_{0.95}S_{1.04})_{\Sigma 1.99}$ to $(Ir_{0.61}Rh_{0.30}Pt_{0.06}Ru_{0.05})_{\Sigma 1.02}(As_{1.01}S_{0.97})_{\Sigma 1.98}$. In contrast, irarsite accompanied by laurite is enriched in Ru (up 8.84 wt.%), with subordinate contents of Rh and Pt (2.96 and 3.88 wt.%, respectively).

Comparison of the compositions of irarasite from the placers and from the chromitite pods from Veluće (Krstić 1993) reveals relative Rh-enrichment in the former. However, the Ru content detected in irarsite from intergrowths with laurite is very similar to that of irarsite inclusions in chromite.

Platarsite

Platarsite has only been observed as small (<10 μm) anhedral grains hosted by irarsite. It is a Rh-poor variety, similar to reported compositions from the Merensky Reef (Tarkian 1987).

Sperrylite

Sperrylite occurs exclusively in rounded and euhedral polyphase inclusions within Ru–Os–Ir alloy, along with other identified PGE arsenides, Pt–Fe and Pt–Cu–Sb alloys. The crystal habit of sperrylite grains within these inclusions ranges from anhedral to euhedral, varying in size between 10 × 5 to 45 × 20 μm. The composition of sperrylite is characterized by significant Ir and Te concentrations, replacing Pt and As, respectively (Table 3). The empirical formulae range from $(Pt_{0.84}Ir_{0.17}Rh_{0.02})_{\Sigma 1.03}(As_{1.85}Te_{0.12})_{\Sigma 1.97}$ to $(Pt_{0.90}Ir_{0.07}Rh_{0.03})_{\Sigma 1.00}(As_{1.93}Te_{0.07})_{\Sigma 2.00}$. Sulfur (0.7 wt.%) was detected only in one case. The concentrations of minor elements are compatible with values recorded in inclusions of sperrylite within chromite in the Hochgrössen ultramafic massif, Austria (Thalhammer & Stumpfl 1988), whereas sperrylite in serpentinized ophiolite from Skyros Island, Greece is pure $PtAs_2$ (Tarkian *et al.* 1992). Sperrylite found in the Shetland ophiolite complex (Prichard & Tarkian 1988) and clinopyroxenite from New South Wales (Johan *et al.* 1989) has an Sb content up to 3 and 21 wt.%, respectively.

Rh–Pd arsenide

After Ru–Os–Ir and Pt–Fe alloys and laurite, Rh–Pd arsenide is the most abundant phase in the samples investigated, being identified in about one-third of the PGM nuggets. Rh–Pd arsenide is commonly associated with Pt–Fe alloy, exhibiting both a morphological and a textural diversity: a) lamellar, lenticular and needle-like crystals are preferentially oriented with respect to the host Pt–Fe alloy; the size of these exsolution blebs is generally less than 50 μm across (Fig. 9C). b) Drop-like inclusions occur in Pt–Fe and Ru–Os–Ir alloys; in the former, they are usually associated either with laths of Ru–Os–Ir and Ru–Ir–Rh alloys or attached to lamellae

TABLE 3. SELECTED ELECTRON-MICROPROBE DATA ON LAURITE, PGE SULFARSENIDES AND PGE ARSENIDES

Analysis No	4	3	46	30	36	48	30	53	58	5	56	40	41
Pt wt. %	<0.10	0.17	0.46	18.11	3.88	50.98	0.49	0.91	9.60	0.84	2.32	14.91	8.48
Os	17.53	0.36	0.77	7.34	<0.10	<0.10	<0.10	<0.10	<0.10	<0.10	<0.10	<0.10	0.12
Ir	6.07	5.72	25.23	19.98	44.47	3.79	<0.10	0.17	0.14	4.92	0.52	29.36	29.87
Ru	39.25	47.81	8.65	6.80	8.84	<0.10	<0.10	<0.10	1.79	21.14	29.92	0.19	0.60
Rh	2.03	5.81	22.43	7.11	2.96	0.93	60.81	40.11	27.22	31.80	26.53	4.06	6.86
Pd	<0.10	<0.10	<0.10	<0.10	<0.10	<0.10	12.65	30.04	37.03	<0.10	0.10	<0.10	<0.10
Fe	nd	nd	nd	nd	nd	<0.10	<0.10	<0.10	<0.10	<0.10	<0.10	<0.10	<0.10
Ni	nd	nd	nd	nd	nd	<0.10	<0.10	<0.10	<0.10	<0.10	<0.10	<0.10	<0.10
Cu	nd	nd	nd	nd	nd	<0.10	<0.10	<0.10	<0.10	<0.10	<0.10	0.26	0.24
S	34.46	33.97	17.56	12.66	14.53	<0.10	<0.10	<0.10	<0.10	<0.10	<0.10	<0.10	<0.10
As	1.02	6.11	24.48	27.96	24.32	42.04	26.04	18.07	25.16	41.39	41.63	26.78	23.82
Sb	nd	nd	nd	nd	nd	<0.10	<0.10	0.40	0.17	<0.10	<0.10	0.21	0.25
Te	<0.10	<0.10	<0.10	<0.10	<0.10	2.77	<0.10	11.96	<0.10	<0.10	<0.10	24.36	29.28
Total	100.36	99.95	99.58	99.96	99.00	100.51	99.99	101.66	101.11	100.09	101.02	100.15	99.52
Atomic proportions													
Pt	-	-	-	0.24	0.05	0.90	0.01	0.01	0.14	0.01	0.02	0.28	0.16
Os	0.17	-	0.01	0.10	-	-	-	-	-	-	-	-	-
Ir	0.06	0.05	0.30	0.27	0.60	0.07	-	-	-	0.05	-	0.56	0.56
Ru	0.72	0.83	0.19	0.18	0.23	-	-	-	0.05	0.38	0.53	0.01	0.02
Rh	0.04	0.10	0.50	0.20	0.08	0.03	1.67	1.15	0.78	0.56	0.46	0.14	0.24
Pd	-	-	-	-	-	-	0.34	0.83	1.03	-	-	-	-
Fe	-	-	-	-	-	-	-	-	-	-	-	-	-
Ni	-	-	-	-	-	-	-	-	-	-	-	-	-
Cu	-	-	-	-	-	-	-	-	-	-	-	0.01	0.01
S	1.97	1.86	1.25	1.04	1.19	-	-	-	-	-	-	-	-
As	0.03	1.14	0.75	0.98	0.85	1.93	0.98	0.71	0.99	1.00	0.99	1.30	1.16
Sb	-	-	-	-	-	-	-	0.01	-	-	-	0.01	0.01
Te	-	-	-	-	-	0.07	-	0.28	-	-	-	0.69	0.83

4 - a euhedral crystal of laurite included in a matrix of Ir-Os-Rh alloy; 3 - subhedral laurite at the margin of Ru-Os-Ir alloy associated with hollingworthite; 46 - hollingworthite in Pt-Fe alloy; 30 - a discrete aggregate of irarsite; 36 - a subhedral grain of irarsite at the grain boundaries of Ru-Os-Ir alloy; 48 - euhedral sperrylite with Rh-Ru arsenide, Pt-Cu-Sb alloy and native platinum, included in Ru-Os-Ir alloy; 30 - a subhedral crystal of Rh-Pd arsenide at the margin of Pt-Fe alloy; 53 - anhedral Rh-Pd arsenide, associated with Ru-Ir-Rh and Ru-Ir-Pt alloys and keithconnite within Pt-Fe alloy; 58 - Rh-Pd arsenide in the polymineralic inclusion within Ru-Os-Ir alloy (Fig. 2D); 5 - a euhedral crystal of Rh-Ru arsenide at the margin of Pt-Fe alloy; 56 - Rh-Ru arsenide in the polyphase inclusion (Fig. 2D); 40, 41 - iridarsenite (?) in an intergrowth with Rh-Ru arsenide along the margin of Ru-Os-Ir alloy; nd - not determined.

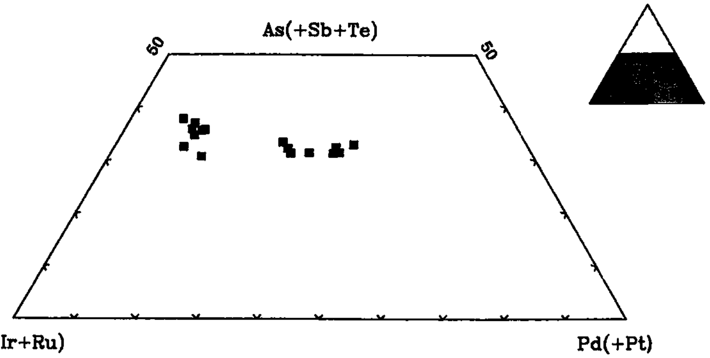

FIG. 10. Compositions of Rh–Pd arsenide (at.%) in the diagram Rh – Pd(+Pt) – As (Sb+Te).

of Ru–Os–Ir alloy; the diameter of these inclusions ranges from 35 to 120 μm (Fig. 9D). c) A subhedral crystal 150 × 120 μm in size replaces a grain of Pt–Fe alloy. Furthermore, Rh–Pd arsenide, set in grains of Ru–Os–Ir alloy, was commonly observed as part of polyphase inclusions. Crystal form within inclusions ranges from subhedral to anhedral; the grains vary in size between 10 and 70 μm across. In reflected light, the Rh–Pd arsenide is pale brownish grey with a green tinge. Bireflectance is distinctive, with a moderate to strong anisotropy. Rotation tints vary from dark brown to pale greyish green.

Selected electron-microprobe data are presented in Table 3. The compositions are close to stoichiometric Me_2As, with variation in Rh/(Rh+Pd) from 0.85 to 0.43 (Fig. 10), although internal chemical zoning has not been observed. Platinum is consistently present, showing a broad variation in content, from 0.35 to 18 wt.%. The Te concentration remains low (<0.2 wt.%), although it reaches 12 wt.% in Rh–Pd arsenide associated with keithconnite. In the majority of grains, As is partially replaced by Sb (up to 3 wt.%). Other minor elements encountered consist of Ru (<0.10–2 wt.%), Ir (<0.10–0.5 wt.%), Cu (<0.10–0.3 wt.%) and Fe (<0.10–0.2 wt.%). In some cases, their presence can be attributed to the surrounding Pt–Fe and Ru–Os–Ir alloys.

The Rh–Pd arsenide from Veluće appears to be the natural equivalent of synthetic β–Rh_2As (orthorhombic, Shunk 1969), with an extensive solid-solution toward monoclinic palladoarsenide (Pd_2As, Begizov *et al.* 1974). Even though the experimental data are sparse for the ternary system Rh–Pd–As, the distinctive optical characteristics and the compositions of the Rh–Pd arsenide suggest that grains with Pd>Rh could hardly be considered as Rh-rich palladoarsenide. Analyses of palladoarsenides from the Oktyabr'sky deposits (Begizov *et al.* 1974) and the Stillwater complex (Cabri *et al.* 1975, Volborth *et al.* 1986) show no Rh and only minor amounts of Pt, Cu, Au, Ag, as well as Sb and Te.

Rh–Ru arsenide

This phase forms a minor constituent, but exhibits diversity of textural relationships with the host Ru–Os–Ir and Pt–Fe alloys. Subhedral to euhedral crystals up to 150 μm across occur at the margin of grains of Pt–Fe and Ru–Os–Ir alloys. They are developed either as single crystals or accompanied by iridarsenite(?). Furthermore, elongate aggregates of subhedral grains and single grains can be found as part of polyphase inclusions within Ru–Os–Ir alloy (Fig. 2D). The largest such aggregate reaches 180 μm across.

A dependence of the optical characteristics on composition is indicated. The Rh–Ru arsenide with Rh/(Rh + Ru) > 0.5 shows strong pleochroism from grey to brownish orange grey; between crossed polars, anisotropy is strong, with blue, dark blue, yellow, yellow-brown to brown rotation tints. On the other hand, a grain with Rh/(Rh + Ru) < 0.5 is greyish brown, with very weak bireflectance. It does not appear to be pleochroic. Its anisotropy is distinct with greyish green, yellowish green and olive-green – brown rotation tints. The Rh-rich members are commonly either simply or polysynthetically twinned.

The compositions of the Rh–Ru arsenide reveal a preponderance of either Rh or, more rarely, Ru (Table 3). The former varies from 23 to 29 at.%, whereas Ru was detected over a range of 26–19 at.%. Other minor elements encountered in Rh–Ru arsenide are Ir (0.14–2.50 at.%), Pt (up to 1 at.%) and traces (≤0.1 wt.%) of Pd, Cu, Fe, Sb and Te. In comparison to the original description of ruthenarsenite (RuAs, Harris 1974) and cherepanovite (RhAs, Rudashevsky *et al.* 1985), the results obtained here differ significantly in both the qualitative optical properties and compositions. Taking into account the isostructural relation and the similar unit-cell parameters of cherepanovite and ruthenarsenite, an extensive solid-solution between RhAs and RuAs end members cannot be ruled out (Fig. 11). This is also indicated by a reported composition

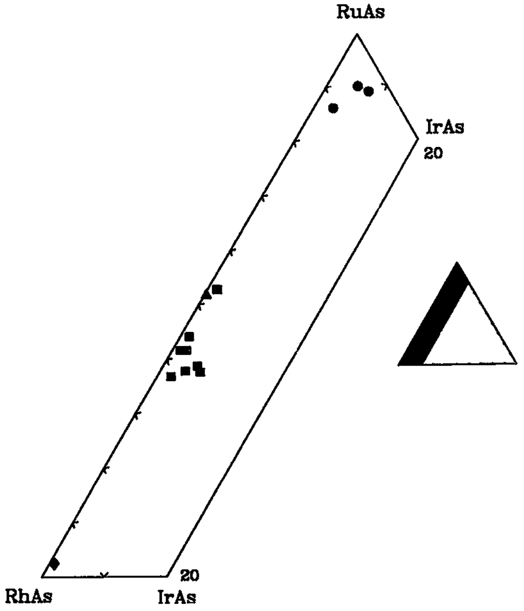

FIG. 11. Compositions of Rh–Ru arsenides (mol.%) in the system RuAs – RhAs – IrAs: ■ this study; ▲ ruthenarsenite from Onverwacht, Transvaal, after Cabri & Laflamme (1981); ● ruthenarsenite from Papua – New Guinea, after Harris (1974); ◆ the average composition of cherepanovite, after Rudashevsky *et al.* (1985).

of ruthenarsenite from Onverwacht, Transvaal, containing 27.4 wt.% Rh (Cabri & Laflamme 1981). However, it cannot be conclusively stated that the Rh–Ru arsenide from Veluće corresponds to a member within an isomorphous series between RhAs and RuAs or represents a new mineral.

Iridarsenite(?) (Ir,Rh,Pt)(As,Te)$_2$

A single aggregate of iridarsenite(?) was observed. It is intergrown with Rh–Ru arsenide and replaces a grain of Ru–Os–Ir alloy. In reflected light, iridarsenite(?) is grey with faint brown tinge and very weak anisotropy. Electron-microprobe analyses reveal the presence of zoning within the aggregate (Table 3); whereas the abundances of Ir are constant (18.52–18.82 at.%), Rh (4.78–8.08 at.%) displays a negative covariation with Pt (9.27–5.25 at.%). The Te content (23.14–27.79 at.%) decreases with increase of the As concentration (43.41–38.67 at.%), clearly indicating Te-for-As substitution. The content of Ru is low and reaches 0.72 at.%.

The composition of iridarsenite from its type locality, Papua – New Guinea (Harris 1974), differs significantly from that recorded here, being enriched in Ir and Ru, and nearly devoid of Te. In spite of the fact that qualitative optical data are similar, speculation as to whether the described phase is a Rh-, Pt- and Te-bearing variety of iridarsenite or possibly a new mineral species requires X-ray confirmation. Reported "sperrylite–iridarsenite" from the Hochgrössen massif, Austria (Thalhammer & Stumpfl 1988) cannot be used *sensu stricto* as an example of extensive $PtAs_2$ – $IrAs_2$ – $RhAs_2$ solid solution because of the high S content (6.5 wt.%) reported. Their composition of "sperrylite–iridarsenite", when recalculated to three atoms per formula unit, corresponds to a structural formula $(Pt_{0.42}Ir_{0.37}Rh_{0.21})_{\Sigma1.00}As_{1.37}S_{0.63}$, and most closely resembles nonstoichometric platarsite (ideally PtAsS). Alternatively, iridarsenite (?) described herein may represent (Ir,Rh,Pt) arsenotelluride. Similarly to the case of grains of RuAsTe and $(Ru,Os)(As,Te,S)_2$ in sulfide ores from the Pechenga ore district (Distler *et al.* 1988), the composition of iridarsenite(?) fits the stoichiometric composition $Me\mathrm{As(Te}_{1-x}\mathrm{As}_x)$, where *Me* is either Ir, Rh and Pt (the present study) or Ru and Os (Distler *et al.* 1988).

Keithconnite

Keithconnite is hosted by a grain of Pt–Fe alloy, where it occurs as anhedral and isometric grains up to 50 × 15 μm in size. They are only seldom isolated; most grains are attached to particles of Ru–Ir–Rh and Ru–Ir–Pt alloy (Fig. 2B). The compositions of the analyzed crystals are consistent and stoichiometrically close to Pd_3Te (Table 4). Minor quantities of other elements, notably Rh, Pt, Sb and Cu, have been detected. The Rh content ranges from 1.8 to 2.7 at.%; Pt and Cu attain 0.7 and 0.6 at.%, respectively, whereas Sb reaches 0.9 at.%. Traces of As, Ir, Ru and Fe also were detected.

Interestingly, a recent investigation of the phase relations in the Pd–Te system did not confirm the existence of Pd_3Te (Kim *et al.* 1990). Instead, the compound $Pd_{20}Te_7$ having trigonal symmetry was reported, with an X-ray pattern different from that of keithconnite.

Pd antimonides

Pd antimonides are rarely present in the PGM assemblage from Veluće. They were discovered as: a) part of polyphase inclusions within Ru–Os–Ir alloy, b) trails of subhedral to euhedral crystals and a vein-like aggregate enclosed by discrete grains of Pt–Fe alloy, and c) irregular patches within an unnamed $(Ru,Rh,Ir)(Te,Sb,As)_2$ mineral, all encapsulated in Ru–Os–Ir alloy.

The compositions of the Pd antimonides from Veluće are given in Table 4; composition 2 is close to the ideal formula of mertieite II, and composition 2a is close to that of mertieite I. As Cabri & Laflamme (1981) have noted, mertieite I and II, and stibiopalladinite can be distinguished from one another only by

TABLE 4. COMPOSITIONS OF KEITHCONNITE, Pd ANTIMONIDES AND UNNAMED (Ru,Ir,Rh)(Te,Sb,As)$_2$

Analysis No.	50	2	2a	1	3
Pt wt. %	0.84	13.94	4.82	5.15	4.15
Os	0.11	< 0.10	< 0.10	< 0.10	< 0.10
Ir	0.40	0.16	< 0.10	5.90	6.66
Ru	0.12	< 0.10	< 0.10	12.73	13.41
Rh	2.47	< 0.10	0.15	9.33	8.79
Pd	66.26	53.13	64.34	< 0.10	< 0.10
Fe	< 0.10	< 0.10	< 0.10	< 0.10	< 0.10
Ni	< 0.10	< 0.10	< 0.10	< 0.10	< 0.10
Cu	0.40	4.05	1.73	0.11	< 0.10
S	< 0.10	< 0.10	< 0.10	< 0.10	< 0.10
As	0.28	0.14	< 0.10	2.38	2.11
Sb	0.70	28.61	29.29	9.60	9.58
Te	28.40	< 0.10	< 0.10	50.39	51.92
Bi	nd	nd	nd	4.64	3.76
Total	99.98	100.03	100.33	100.23	100.38
			Atomic proportions		
Pt	0.02	0.90	0.41	0.10	0.08
Os	-	-	-	-	-
Ir	0.01	0.01	-	0.11	0.13
Ru	-	-	-	0.47	0.49
Rh	0.11	-	0.02	0.34	0.32
Pd	2.79	6.90	10.09	-	-
Fe	-	-	-	-	-
Ni	-	-	-	-	-
Cu	0.03	0.81	0.47	0.01	-
S	-	-	-	-	-
As	0.02	0.02	-	0.12	0.11
Sb	0.02	2.96	4.01	0.29	0.29
Te	1.00	-	-	1.48	1.51
Bi	-	-	-	0.08	0.07

50 - an inclusion of keithconnite within Pt-Fe alloy (Fig. 2B); 2 - Pd antimonide traversing unnamed (Ru,Rh,Ir)(Te,Sb,As)$_2$; 2a - Pd antimonide within Pt-Fe alloy; 1,3 - unnamed (Ru,Rh,Ir)(Te,Sb,As)$_2$ hosted by Ru-Os-Ir alloy; nd - not determined.

X-ray diffraction. However, regardless of the *Me*:(Sb,As) value, the Pd antimonides from Veluće display relatively high abundances of Pt (up to 17.5 wt.%) and Cu (up to 4 wt.%).

Unnamed (Ru,Rh,Ir)(Te,Sb,As)$_2$

Two grains of this unnamed phase have been found as inclusions in a grain of Ru–Os–Ir alloy. One grain is subhedral in form and reaches 70 × 45 μm in size. It is traversed by irregular patches of Pd antimonide and is adjoined by an anhedral grain of Pt–Fe alloy. The second grain rims laurite and is intergrown with a grain of Pt–Fe alloy. In reflected light, this mineral is grey with a faint brownish tinge and displays no anisotropy. Its reflectivity is slightly higher than that of laurite.

Electron-microprobe data reveal a MeX_2 stoichiometry, where *Me* = Ru, Rh, Ir and Pt, and *X* = Te, Sb, As and Bi (Table 4). The composition is homogeneous and varies from $(\mathrm{Ru}_{0.47}\mathrm{Rh}_{0.34}\mathrm{Ir}_{0.11}\mathrm{Pt}_{0.10}\mathrm{Cu}_{0.01})_{\Sigma 1.03}(\mathrm{Te}_{1.48}\mathrm{Sb}_{0.29}\mathrm{As}_{0.12}\mathrm{Biv}_{0.08})_{\Sigma 1.97}$ to $(\mathrm{Ru}_{0.49}\mathrm{Rh}_{0.32}\mathrm{Ir}_{0.13}\mathrm{Pt}_{0.08})_{\Sigma 1.02}(\mathrm{Te}_{1.51}\mathrm{Sb}_{0.29}\mathrm{As}_{0.11}\mathrm{Bi}_{0.07})_{\Sigma 1.98}$. In comparison, optically similar, unnamed Rh(Te,Bi)$_2$ in Pt–Fe nuggets from Ethiopia contains no Ru and considerably more Bi (Cabri *et al.* 1981).

Ruthenium oxide(?)

A fine-grained phase, occurring as a pseudomorph after several grains of laurite, was identified. In reflected light, this mineral is dark grey with a faint brownish tinge, and strongly bireflectant and anisotropic, with rotation colors that range from dark grey to bronze-yellow.

Electron-microprobe analyses of this phase show low analytical totals (Table 5). The compositions reveal abundant Ru, which varies from 49 to 57 wt.%. Other PGE were recorded in relatively low amounts, the most enriched being Os (up to 6 wt.%), whereas Ir remains at a rather low level (2–3 wt.%). Rhodium reaches 3 wt.%, and Pt is ≤0.5 wt.%. An unusually high content of Hg (8–10 wt.%) is most likely due to amalgamation. The concentration of Fe varies between 5 and 10 wt.%. Other elements (S, As, Sb, Cu, Ni, Co, Ca) are present in negligible quantities (below 0.7 wt.%). Recalculation of the compositions into oxide components provides a clue that this phase appears to be RuO$_2$. However, at the moment we cannot rule out the presence of OH.

A similar greyish anisotropic secondary phase after laurite with Ru >> Os > Mg > Si >> Fe has been reported by Cabri & Genkin (1991) in lode PGM deposits from the Urals.

Gold

Native gold occurs as discrete, irregular and dendritic grains. Intergrowths of the gold and the PGM have not been found. Minerals encountered in the gold as inclusions and marginal replacement are pyrite, galena and quartz. The gold is characterized by relatively uniform composition: Ag varies from 7 to 11 wt.%, whereas Cu remains low, with maximum content of 0.25 wt.%. The PGE are systematically below detection limits. There is a striking compositional difference between the core and the white, high-reflectance rim along some grains. The rim carries a high concentration

TABLE 5. CHEMICAL COMPOSITION OF RuO_2

Analysis No.	1	2
Pt wt. %	0.10	< 0.10
Os	5.87	1.55
Ir	3.72	2.87
Ru	49.62	56.68
Rh	0.71	< 0.10
Pd	< 0.10	< 0.10
Fe	8.68	8.08
Ni	0.41	< 0.10
Co	0.18	< 0.10
Ca	0.68	< 0.10
Hg	8.21	10.15
S	0.15	< 0.10
As	0.23	< 0.10
Total	78.56	79.33

Recalculated composition		
PtO_2	0.16	-
OsO_2	6.86	1.81
IrO_2	4.34	3.35
RuO_2	65.33	74.62
RhO_2	0.93	-
PdO_2	-	-
FeO	11.17	10.39
NiO	0.52	-
CoO	0.22	-
CaO	1.22	-
HgO	8.87	10.96
SO_2	0.30	-
As_2O_3	0.37	-
Total	100.25	101.13

1 RuO_2 pseudomorph after lenticular grain of laurire within Ru-Os-Ir alloy. 2 RuO_2 replacing euhedral grain of laurite.

of Hg (34–35 wt.%), whereas the Ag content is 0.4 wt.%. The high abundance of Hg presumably reflects dissolution by amalgamation.

Auriferous quartz–pyrite veins in the Paleozoic schists and the Cretaceous sediments are the most likely source of the gold found in the placer deposits. On the basis of the discovery of gold in the rivers that pass exclusively through the Cretaceous sediments, Pašić & Maksimović (1952) proposed this origin for the gold in the placers.

Silicate inclusions in nuggets

Inclusions of primary and secondary silicates, occurring as small (<50 μm across), subhedral grains, have rarely been found within grains of Ru–Os–Ir alloy. Olivine, as the only primary silicate inclusion, represents the most abundant silicate phase hosted by the Ru–Os–Ir alloy. The composition of olivine is fairly uniform, extending from $Fo_{92.0}$ to $Fo_{92.4}$, and closely matches that of olivine from the Veluće dunite ($Fo_{92.2}$ to $Fo_{92.7}$). The inclusions of secondary silicate minerals are very rare and consist of serpentine, Fe-rich chlorite and trace amounts of quartz. These inclusions presumably represent the products of subsequent supergene alteration of primary silicates. Krstić (1993) has shown that assemblages of high-temperature silicate inclusions are common in chromite from the Veluće ophiolite and comprise magnesio-, magnesio-hastingsitic and edenitic hornblende [nomenclature after Leake (1978)], Na-rich phlogopite with $0.90 < Mg\# < 0.96$ and $0.51 < Na/(Na + K) < 0.87$, olivine ($Fo_{95} - Fo_{96}$) and orthopyroxene ($En_{96} - En_{96.5}$).

DISCUSSION

Many recent studies provide convincing mineralogical and geochemical evidence for the primary, magmatic formation of PGM nuggets and their concentration in placers by mechanical processes of transport (Hagen *et al.* 1990, Johan *et al.* 1990, Nixon *et al.* 1990, Slansky *et al.* 1991, Augé & Legendre 1992, Peck *et al.* 1992, Weiser & Schmidt-Thomé 1993, Augé & Maurizot 1995). Furthermore, examination of Os isotope ratios of PGM nuggets from a variety of placers has shown the lack of significant isotopic heterogeneity in individual grains, which strongly suggests a mantle signature and a high-temperature origin (Hattori *et al.* 1992, Hattori & Cabri 1992). Contrary to these results, low-temperature growth of PGM nuggets has been proposed by Augustithis (1965), Cousins (1973), Cousins & Kinloch (1976) and Bowles (1986, 1988, 1990); these authors deduced this mode of origin primarily on the basis of grain-size discrepancies between PGM from the primary deposits and placers, as well as some morphological peculiarities of PGM nuggets, although in most cases, the characteristics of primary PGE mineralization in assumed source-rocks are unknown. In this manner, the Veluće area, with its established occurrences of PGM in chromitite, could provide important information related to provenance of the PGM in spatially associated placers.

The relative abundance and composition of the primary PGM in chromitite (Krstić 1993) are consistent with those in the placers. The Ru–Os–Ir alloy represents the major PGM in both assemblages, exhibiting overlap in compositional ranges (Fig. 3). Minor elements encountered in these populations of alloy also attain similar concentrations. In addition, the compositions of laurite in chromitite are comparable with those in the placers, including the conspicuous enrichment in Rh and As, as well as comparable quantities of Pt. The chemistry of the irarsite solid-solution in chromitite pods matches that of irarsite in the placers, although in general, there is more Rh and less Ru in the latter. The similarity in compositions between the primary and alluvial PGM suggests an origin from a common magmatic source related to the ultramafic section of the Veluće ophiolite. Assuming that Cu increases and Ni decreases toward the top of an ophiolite sequence (Lord & Prichard 1989, Prichard & Lord 1990), the higher Cu/Ni value encountered in the alluvial Ru–Os–Ir alloy compared to that in primary grains enclosed by chromite may indicate derivation of the former from a slightly higher stratigraphic level, compared to the PGM-bearing chromitite horizons studied by Krstić (1993).

However, there are obvious discrepancies in the grain size, mode of occurrence and nature of the mineral phases identified between the PGM assemblages in chromitites *versus* those from the placers. Typically, PGM in chromitites are included in chromite and do not exceed 12 μm. Only a single aggregate of irarsite grains, set in a silicate matrix of chromitite, does exceed this size (30 μm across). In contrast, grains of Ru–Os–Ir and Pt–Fe alloys described here can reach 5 mm in diameter. Finally, the quite pronounced diversity of the PGM phases in placers contrasts with the relatively simple PGM assemblages in chromitite (Krstić 1993). The observed differences between the primary and placer occurrences could be attributed to limited sampling of the former. Furthermore, derivation of PGM nuggets from eroded, high-grade primary occurrences may also account for the mineralogical and compositional gap between PGE mineralization in bedrock and spatially associated placers, as was suggested by Nixon *et al.* (1990).

The textural relationships of the PGM described herein also constrain the conditions during formation of the PGE mineralization in the placers. The presence of euhedral laurite and droplet-like inclusions of Pt–Fe alloy within Ru–Os–Ir alloy implies high-temperature crystallization of the PGM. Likewise, the simplectitic intergrowth of rutheniridosmine with Ru–Ir–Pt alloy (Fig. 2C) and the exsolution of lamellae of Pt–Fe alloy within the host Ru–Os–Ir alloy are in good agreement with a magmatic origin of PGM. High-temperature formation of the PGM assemblage is also illustrated by: a) exsolution-induced textures of Ir–Os–Rh alloy members with included euhedral crystals of laurite, b) occurrences of polymineralic grains consisting of Ru–Os–Ir and Pt–Fe alloys whose textures are attributed to breakdown of a once-homogeneous Ru–Os–Ir–Pt–Fe compound during cooling, c) exsolution of Ru–Ir–Pt and Ru–Os–Ir alloys within Pt–Fe alloy, and d) symplectitic intergrowths of Pt–Fe and Ru–Os–Ir alloys. Finally, inclusions of olivine within Ru–Os–Ir alloy, with the compositions very similar to those in dunite from the Veluće ophiolite, leave little doubt that placer nuggets have crystallized in a high-temperature, magmatic environment.

The origin of PGE-bearing arsenides is still controversial. Two hypotheses have been advanced to explain examples of PGE sulfarsenides and arsenides in ophiolite complexes: a) they are the primary phases, formed during the magmatic stage (Prichard & Tarkian 1988, Gervilla & Leblanc 1990, Edwards 1990, Gervilla *et al.* 1996), or b) they are secondary and hydrothermal in origin, reflecting late introduction of As during low-temperature alteration of ultramafic rocks (Thalhammer & Stumpfl 1988, Corrivaux & Laflamme 1990, Prichard *et al.* 1994).

There are several reasons to believe that the former view can account for the genesis of PGE sulfarsenides and arsenides in the Veluće ophiolite. The globular inclusions of Rh–Pd and Rh–Ru arsenides and sperrylite embedded in Ru–Os–Ir alloy described here seem to be formed from an As–, Rh–, Pd– and Pt–bearing magmatic liquid, trapped during growth of the alloy grains. Seldom observed euhedral crystals of sperrylite suggest that its crystallization could even precede that of the host grains of alloy. The same timing is proposed for the polyphase inclusions made up of Rh–Pd and Rh–Ru arsenides and Pt–Cu (± Sb) alloys. Their irregular crystal habit would be difficult to explain by crystallization from a trapped PGE-rich liquid. Moreover, the presence of preferentially oriented Rh–Pd arsenide and Pd antimonides with respect to the host Pt–Fe alloy must be caused by an unmixing process. The compositions of these exsolution-induced blebs suggest complex Pt–Fe–Rh–Pd–As–Sb solid solutions that existed at magmatic temperatures. Subhedral to euhedral crystals of hollingworthite, irarsite, Rh–Pd arsenide, Rh–Ru arsenide and iridarsenite (?) found at the margin of the Ru–Os–Ir and Pt–Fe alloys are considered to have formed at the final stage of growth of the alloy grains.

Although the euhedral morphology of laurite inclusions at the periphery of Ru–Os–Ir alloy contra-indicates a hydrothermal origin (Augé & Legendre 1992), a few grains of alloy clearly demonstrate alteration-related features. These are replaced along the margin and cleavages by fine-grained laurite (Fig. 9B), which is locally accompanied by hollingworthite and irarsite. Laurite formation during serpentinization has been envisaged for grains hosted by the silicate matrix of chromitites in the Troodos ophiolite (McElduff & Stumpfl 1990), and marginal replacement of Ru–Os–Ir alloy by laurite was noted in placers from Burma (Hagen *et al.* 1990). However, the magnetite–awaruite assemblage in dunite and serpentinized silicate matrix of chromitites from Veluće (Krstić 1993) is evidence of low $f(S_2)$ and $f(O_2)$ during serpentinization (Eckstrand 1975), which does not favor precipitation of laurite and PGE sulfarsenide under these conditions. Thus, replacement of Ru–Os–Ir alloy by the secondary phases may coincide with alteration subsequent to serpentinization. The development of ruthenium oxide (?) as the pseudomorph after laurite is probably related to conditions of elevated $f(O_2)$ during weathering of the bedrock.

It is now widely recognized that a sulfide liquid has a dominant role in concentrating PGE in layered intrusions (Campbell *et al.* 1983, Naldrett *et al.* 1990). Alternatively, several studies of PGM mineralization in layered igneous complexes propose the transport and concentration of PGE by hydrous, chloride-rich fluid (Ballhaus & Stumpfl 1986, Boudreau *et al.* 1986, Stumpfl 1986, Boudreau & McCallum 1992). Considering the absence of base-metal sulfides in the PGM assemblages examined here and the low Ni content of the PGM, it seems unlikely that the sulfide liquid model could account for the observed PGM. The latter genetic model, postulating the formation of the PGM from high-temperature hydrothermal activity, is inconsistent with the mineralogy and textural features of the PGM described above. The abundance of refractory PGE alloys in the PGM assemblage, as well as the widespread occurrences of drop-like inclusions of PGM within Ru–Os–Ir alloy, argue against a crucial role played by a fluid phase in the concentration of PGE in the placers associated with the Veluće ophiolite. At this stage of the research, we suggest that the textural and chemical results presented indicate the crystallization of PGM from a silicate melt, with an important role of As, Sb and Te in deposition of PGE. This interpretation is supported by recent studies by Peck *et al.* (1992), who concluded that PGE alloys and complex PGE–As–Te–Bi compounds have very low solubility in silicate melts, and in certain type of magmas (Si- and Mg-rich, S-poor), they can precipitate directly as cumulus phases from the parental silicate liquid.

CONCLUSIONS

Mineralogical studies of the PGM in gold-bearing placers from the Veluće area, Yugoslavia, show the predominance of Ru–Os–Ir and Pt–Fe alloys that may contain a diversity of other PGE-bearing species as exsolution-induced blebs and inclusions. The compositions of phases studied indicate crystallization from a Ru- and Pt-bearing liquid, with variable contents of other PGE, most notably Rh. The preponderance of PGE alloys and the absence of base-metal sulfides in the PGE mineralization, as well as a rather low average concentration of Os in laurite, suggest a relatively low $f(S_2)$ during precipitation of the PGM assemblages. Instead, a significant involvement of As, Sb and Te in the segregation of the PGE is suggested.

The textural features among the PGM are testimony to a primary origin, linked to direct crystallization from a high-temperature silicate melt. Secondary evolution of the PGM at low temperatures (<400–500°C) is limited to replacement of Ru–Os–Ir alloy by laurite, hollingworthite and irarsite, and alteration of laurite under locally high $f(O_2)$.

The compositional similarity of the PGM in the Veluće chromitites with those from nearby placers argues for a common source, represented by the ultramafic section of the ophiolite. The observed discrepancies in grain size and mineralogy between the PGM in lode and placer assemblages could be rationalized either as an artifact of insufficient knowledge of the former or complete erosion of high-grade, bedrock occurrences of PGM. The origin of gold in the placers is likely related to erosion of vein-type mineralization in the Paleozoic schists and Cretaceous sediments.

ACKNOWLEDGEMENTS

Special thanks are extended to Prof. Z. Maksimović of the University of Belgrade, who initiated this study and kindly provided PGM and gold grains from his personal collection. We are very grateful to Mrs. B. Cornelisen for patient and careful work in connection with the electron-microprobe analyses. Dr. A. Popević's generosity in providing access to the geological map and technical reports is acknowledged. We thank Dr. Lj. Cvetković of the University of Belgrade for preparing some polished sections. The authors sincerely appreciate the thorough reviews by Drs. D.C. Peck and A.M. McDonald, whose suggestions greatly improved and strengthened this manuscript. Dr. R.F. Martin is thanked for his invaluable editorial comments and efficiency. Funding for a one-month stay for the senior author at the University of Hamburg was provided by Mr. D. Milinović and Mrs. S. Milinović of EGAL DM Ltd., Valjevo, Yugoslavia.

REFERENCES

AUGÉ, T. & LEGENDRE, O. (1992): Pt–Fe nuggets from alluvial deposits in eastern Madagascar. *Can. Mineral.* **30**, 983-1004.

________ & MAURIZOT, P. (1995): Stratiform and alluvial platinum mineralization in the New Caledonia ophiolite complex. *Can. Mineral.* **33**, 1023-1045.

AUGUSTITHIS, S.S. (1965): Mineralogical and geochemical studies of the platiniferous dunite – birbirite – pyroxenite complex of Yubdo, Birbir, W. Ethiopia. *Chem. Erde* **24**, 159-196.

BALLHAUS, C.G. & STUMPFL, E.F. (1986): Sulfide and platinum mineralization in the Merensky Reef: evidence from hydrous silicates and fluid inclusions. *Contrib. Mineral. Petrol.* **94**, 193-204.

BEGIZOV, V.D., MESHCHANIKOVA, V.I. & DUBAKINA, L.S. (1974): Palladoarsenide, Pd_2As, a new natural palladium arsenide from the copper–nickel ores from the Oktyabr'sky deposits. *Zap. Vses. Mineral. Obshchest.* **103**, 104-107 (in Russ.).

Boudreau, A.E., Mathez, E.A. & McCallum, I.S. (1986): The halogen geochemistry of the Stillwater and Bushveld complexes: evidence for transport of the platinum-group elements by Cl-rich fluids. *J. Petrol.* **27**, 967-986.

________ & McCallum, I.S. (1992): Concentration of platinum-group elements by magmatic fluids in layered intrusions. *Econ. Geol.* **87**, 1830-1848.

Bowles, J.F.W. (1986): The development of platinum-group minerals in laterites. *Econ. Geol.* **81**, 1278-1285.

________ (1988): Further studies of the development of platinum-group minerals in the laterites of the Freetown layered complex, Sierra Leone. *In* Geo-Platinum '87 (H.M. Prichard, P.J. Potts, J.W.F. Bowles & S.J. Cribb, eds.). Elsevier Applied Science, London, U.K. (273-280).

________ (1990): Platinum–iron alloys, their structural and magnetic characteristics in relation to hydrothermal and low-temperature genesis. *Mineral. Petrol.* **43**, 37-47.

Burgath, K.-P. (1988): Platinum-group minerals in ophiolitic chromitites and alluvial placers deposits, Meratus–Bobaris area, southeast Kalimantan. *In* Geo-Platinum '87 (H.M. Prichard, P.J. Potts, J.W.F. Bowles & S.J. Cribb, eds.). Elsevier Applied Science, London, U.K. (383-403).

Cabri, L.J., Criddle, A.J., Laflamme, J.H.G., Bearne, G.S. & Harris, D.C. (1981): Mineralogical study of complex Pt–Fe nuggets from Ethiopia. *Bull. Minéral.* **104**, 508-525.

________ & Genkin, A.D. (1991): Re-examination of Pt alloys from lode and placers deposits, Urals. *Can. Mineral.* **29**, 419-425.

________ & Laflamme, J.G.H. (1981): Analyses of minerals containing platinum-group elements. *In* Platinum-Group Elements: Mineralogy, Geology, Recovery (L.J. Cabri, ed.). *Can. Inst. Min. Metall., Spec. Vol.* **23**, 151-173.

________, ________, Stewart, J.M., Rowland, J.F. & Chen, T.T. (1975): New data on some palladium arsenides and antimonides. *Can. Mineral.* **13**, 321-335.

Campbell, I.H., Naldrett, A.J. & Barnes, S.J. (1983): A model for the origin of the platinum-rich sulfide horizons in the Bushveld and Stillwater Complexes. *J. Petrol.* **24**, 133-165.

Corrivaux, L. & Laflamme, J.H.G. (1990): Minéralogie des éléments du groupe du platine dans les chromitites de l'ophiolite de Thetford Mines, Québec. *Can. Mineral.* **28**, 579-595.

Cousins, C.A. (1973): Notes on geochemistry of the platinum-group elements. *Trans. Geol. Soc. S. Afr.* **76**, 77-81.

________ & Kinloch, E.D. (1976): Some observations on textures and inclusions in alluvial platinoids. *Econ. Geol.* **71**, 1377-1398.

Dick, H.J.B. & Bullen, T. (1984): Chomian spinel as a petrogenetic indicator in abyssal and alpine-type peridotites and spatially associated lavas. *Contrib. Mineral. Petrol.* **86**, 54-76.

Ding, Kuishou (1980): Further studies of the minerals "isoplatin copper" and "hongshiite". *Sci. Geol. Sinica* **2**, 168-171 (in Chinese).

Distler, V.V., Grokhovskaya, T.L., Evstigneeva, T.L., Sluzenikin, S.F., Filiminova, A.A., Djuzikov, O.A. & Laputina, I.P. (1988): *Petrology of Sulfide Magmatic Ore Formation.* Nauka, Moskow, Russia (in Russ.).

Eckstrand, O.R. (1975): The Dumont serpentinite: a model for control of nickeliferous opaque mineral assemblages by alteration reactions in ultramafic rocks. *Econ. Geol.* **70**, 183-201.

Edwards, S.J. (1990): Harzburgites and refractory melts in the Lewis Hills massif, Bay of Island ophiolite complex: the base-metals and precious metals story. *Can. Mineral.* **28**, 537-552.

Feather, C.E. (1976): Mineralogy of platinum-group minerals in the Witwatersrand, South Africa. *Econ. Geol.* **71**, 1399-1428.

Ford, R.J. (1981): Platinum-group minerals in Tasmania. *Econ. Geol.* **76**, 498-504.

Gervilla, F. & Leblanc, M. (1990): Magmatic ores in high-temperature Alpine-type lherzolite massifs (Rhonda, Spain and Beni Bousera, Morocco). *Econ. Geol.* **85**, 112-132.

________, ________, Torres-Ruiz, J. & Hach-Alí, P.F. (1996): Immiscibility between arsenide and sulfide melts: a mechanism for the concentration of noble metals. *Can. Mineral.* **34**, 485-502.

Hagen, D., Weiser, T. & Htay, T. (1990): Platinum-group minerals in Quaternary gold placers in the Upper Chindwin area of northern Burma. *Mineral. Petrol.* **42**, 265-286.

Harris, D.C. (1974): Ruthenarsenite and iridarsenite, two new minerals from the Territory of Papua and New Guinea and associated irarsite, laurite and cubic iron-bearing platinum. *Can. Mineral.* **12**, 280-284.

________ & Cabri, L.J. (1973): The nomenclature of the natural alloys of osmium, iridium and ruthenium based on new compositional data of alloys from world-wide occurrences. *Can. Mineral.* **12**, 104-112.

________ & ________ (1991): Nomenclature of platinum-group-element alloys: review and revision. *Can. Mineral.* **29**, 231-237.

Hattori, K., Burgath, K.-P. & Hart, S.R. (1992): Os-isotope study of platinum-group minerals in chromitites in Alpine-type ultramafic intrusions and the associated placers in Borneo. *Mineral. Mag.* **56**, 157-164.

________ & Cabri, L.J. (1992): Origin of platinum-group-mineral nuggets inferred from an osmium-isotope study. *Can. Mineral.* **30**, 289-301.

Irvine, T.N. (1965): Chromian spinel as a petrogenetic indicator. 1. Theory. *Can. J. Earth Sci.* **2**, 648-672.

Johan, Z., Ohnenstetter, M., Fischer, W. & Amosse, J. (1990): Platinum-group minerals from the Durance River alluvium, France. *Mineral. Petrol.* **42**, 287-306.

________, ________, Slansky, E., Barron, L.M. & Suppel, D. (1989): Platinum mineralization in the Alaskan-type intrusive complexes near Fifield, New South Wales, Australia. 1. Platinum-group minerals in clinopyroxenites of the Kelvin Grove prospect, Owendale Intrusion. *Mineral. Petrol.* **40**, 289-309.

Karamata, S. (1988): Ophiolitic zones in Yugoslavia: origin and significance for the interpretation of geological evolution of Yugoslavia. *Bull. Acad. Serbe Sci. Arts* **52**, 95-110 (in Serbian).

________, Majer, V. & Pamić, J. (1980): Ophiolites of Yugoslavia. *In* Tethyan Ophiolites (G. Rocci, ed.). *Spec. Issue* **1**, 105-124.

Kim, Won-Sa, Chao, G.Y. & Cabri, L.J. (1990): Phase relations in the Pd–Te system. *J. Less-Common Metals* **162**, 61-74.

Krstić, S. (1993): *Ore Minerals from the Veluće Area.* M.Sc. thesis, Univ. Belgrade, Belgrade, Yugoslavia (in Serbian).

Leake, B.E. (1978): Nomenclature of amphiboles. *Can. Mineral.* **16**, 501-520.

Legendre, O. & Augé, T. (1986): Mineralogy of platinum-group mineral inclusions in chromitites from different ophiolitic complexes. *In* Metallogeny of Basic and Ultrabasic Rocks (M.J. Gallagher, R.A. Ixer, C.R. Neary & H.M. Prichard, eds.). Institution of Mining and Metallurgy, London, U.K. (361-372).

Lord, R.A. & Prichard, H.M. (1989): An igneous source for gold in the Shetland ophiolite. *Trans. Inst. Mining Metall.* **98**, B44-B46.

Maksimović, Z. (1981): Types of the fossil weathering of ultramafic rocks in SE Europe. *Bull. Acad. Serbe Sci. Arts* **21**, 13-26.

________ (1992): Geochemistry of ultramafites and associated ore deposits. *Bull. Sci. Invest.* **17**, 54 (in Serbian).

Mao, Shuite & Zhou, Xueci (1989): Iridrhoruthenium and its matrix mineral-isoferroplatinum. *Acta Mineral. Sinica* **9**, 136-140 (in Chinese).

McElduff, B. & Stumpfl, E.F. (1990): Platinum-group minerals from the Troodos ophiolite, Cyprus. *Mineral. Petrol.* **42**, 211-232.

Naldrett, A.J., Brügmann, G.E. & Wilson, A.H. (1990): Models for the concentration of PGE in layered intrusions. *Can. Mineral.* **28**, 389-408.

Nixon, G.T., Cabri, L.J. & Laflamme, G.J.H. (1990): Platinum-group-element mineralization in lode and placer deposits associated with the Tulameen Alaskan-type complex, British Columbia. *Can. Mineral.* **28**, 503-535.

Pašić, M. & Maksimović, Z. (1952): Résultats des recherches géologiques et minéralogiques des environs de village de Veluće au Sud-Est de Trstenik (Serbie Occidentale), avec vue speciale sur les apparitions minières. *Zbor. rad. SAN- u* **XXIII**, **4**, 53-88 (in Serbian with abstract in French).

Peck, D.C., Keays, R.R. & Ford, R.J. (1992): Direct crystallization of refractory platinum-group element alloys from boninitic magmas: evidence from western Tasmania. *Aust. J. Earth Sci.* **39**, 373-387.

Popević, A. (1990): *The Report of Basic Geological Investigation of Chromites from Veluće in 1989.* DP "IMS", Belgrade (in Serbian).

________ (1991): *The Report of Basic Geological Investigation of Chromites from Veluće in 1990.* DP "Geozavod-IMS", Belgrade (in Serbian).

Prichard, H.M., Ixer, R.A., Lord, R.A., Maynard, J. & Williams, N. (1994): Assemblages of platinum-group minerals and sulfides in silicate lithologies and chromite-rich rocks within the Shetland ophiolite. *Can. Mineral.* **32**, 271-294.

________ & Lord, R.A. (1990): Platinum and palladium in the Troodos ophiolite complex, Cyprus. *Can. Mineral.* **28**, 607-617.

________ & Tarkian, M. (1988): Platinum and palladium minerals from two PGE-rich localities in the Shetland ophiolite complex. *Can. Mineral.* **26**, 979-990.

Roeder, P.L. & Campbell, I.H. (1985): The effect of post-cumulus reactions on composition of chrome spinels from the Jimberlana intrusion. *J. Petrol.* **26**, 763-786.

Rudashevsky, N.S., Mochalov, A.G., Trubkin, N.N., Shumskaya, N.I., Shkursky, V.I. & Evstigneeva, T.L. (1985): Cherepanovite, RhAs – a new mineral. *Zap. Vses. Mineral. Obshchest.* **114**, 464-469 (in Russ.).

Shunk, F.A. (1969): *Constitution of Binary Alloys* (2nd Supplement). McGraw-Hill, New York, N.Y.

Slansky, E., Johan, Z., Ohnenstetter, M., Barron, L.M. & Suppel, D. (1991): Platinum mineralization in the Alaskan-type intrusive complexes near Fifield, N.S.W., Australia. 2. Platinum-group minerals in placer deposits at Fifield. *Mineral. Petrol.* **43**, 161-180.

Stumpfl, E.F. (1986): Distribution, transport and concentration of platinum-group elements. *In* Metallogeny of Basic and Ultrabasic Rocks (M.J. Gallagher, R.A. Ixer, C.R. Neary & H.M. Prichard, eds.). Institution of Mining and Metallurgy, London, U.K. (379-394).

________ & Tarkian, M. (1976): Platinum genesis: new mineralogical evidence. *Econ. Geol.* **71**, 1451-1460.

Tarkian, M. (1987): Compositional variations and reflectance of the common platinum-group minerals. *Mineral. Petrol.* **36**, 169-190.

________, Economou-Eliopoulos, M. & Eliopoulos, D.G. (1992): Platinum-group minerals and tetraauricupride in ophiolitic rocks of Skyros Island, Greece. *Mineral. Petrol.* **47**, 55-66.

THALHAMMER, O.A.R. & STUMPFL, E.F. (1988): Platinum-group minerals from Hochgrössen ultramafic massif, Styria: first reported occurrence of PGM in Austria. *Trans. Inst. Mining Metall.* **97**, B77-B82.

THAYER, T.P. (1970): Chromite segregations as petrogenetic indicators. *Geol. Soc. S. Afr., Spec. Publ.* **1**, 380-390.

TOMA, S.A. & MURPHY, S. (1977): The composition and properties of some native platinum concentrates from different localities. *Can. Mineral.* **15**, 59-69.

TÖRNROOS, R. & VUORELAINEN, Y. (1987): Platinum-group metals and their alloys in nuggets from alluvial deposits in Finnish Lapland. *Lithos* **20**, 491-500.

URASHIMA, Y., WAKABAYASHI, T., MASAKI, T. & TERASAKI, Y. (1974): Ruthenium, a new mineral from Horokanai, Hokkaido, Japan. *Mineral. J. Japan* **7**, 438-444.

VOLBORTH, A., TARKIAN, M., STUMPFL, E.F. & HOUSLEY, R.M. (1986): A survey of the Pd–Pt mineralization along the 35-km strike of the J–M Reef, Stillwater Complex, Montana. *Can. Mineral.* **24**, 329-346.

WEISER, T. & SCHMIDT-THOMÉ, M. (1993): Platinum-group minerals from the Santiago River, Esmeraldas Province, Ecuador. *Can. Mineral.* **31**, 61-73.

Received February 9, 1996, revised manuscript accepted October 21, 1996.